

ULTRA-WIDE BANDGAP MATERIALS, DEVICES, AND SYSTEMS



Theoretical characterization and computational discovery of ultra-wide-band-gap semiconductors with predictive atomistic calculations

Emmanouil Kioupakis^{1,a)}, Sieun Chae¹, Kyle Bushick¹, Nick Pant^{1,2}, Xiao Zhang¹, Woncheol Lee³

Received: 26 August 2021; accepted: 11 November 2021; published online: 30 November 2021

First-principles calculations based on density-functional theory have become an established theoretical characterization toolkit to understand and predict the structural and functional properties of materials. In this work, we review recent methodological developments and applications of density-functional theory techniques that relate to the study of ultra-wide-band-gap semiconductors. The topics we cover are directly relevant to the fabrication and operation of devices, such as the stability, synthesis, and doping of semiconductors, along with a survey of work relating to their charge and heat transport, optical properties, and carrier recombination. We further address how high-throughput calculations and materials-informatics techniques can aid the discovery of new ultra-wide-band-gap semiconducting materials with targeted functionalities. Our review highlights how density-functional theory techniques can work in tandem with experiment to advance the state of the art in ultra-wide-band-gap semiconductor research.

Introduction to ultra-wide-band-gap semiconductors

Ultra-wide-band-gap (UWBG) semiconductors, i.e., semiconducting materials with gaps wider than GaN (3.5 eV), have recently emerged as an area of intensive research for electronic and optoelectronic applications [1]. Their ultra-wide gaps allow them to tolerate high electric fields without suffering dielectric breakdown, enabling high-power and high-frequency electronic devices for telecommunications, electric vehicles, and smart electricity grids. In addition, light emission from ultra-widegap materials occurs in the deep ultraviolet part of the electromagnetic spectrum (UV-C), which damages DNA molecules very effectively and enables sterilization and water purification based on solid-state devices. Several UWBG semiconductors are being explored for device applications, with most efforts focusing on diamond, cubic boron nitride (c-BN), aluminum-gallium nitride alloy ($Al_xGa_{1-x}N$), and the β polytype of gallium oxide $(\beta$ -Ga₂O₃) (Fig. 1). The extensive research activity on these materials is motivated by their experimentally demonstrated reasonable performance in unipolar majority-carrier field-effect transistors and/or UV light-emitting devices.

However, despite decades of research, only this handful of UWBG semiconductors have been developed to date and they are all affected by intrinsic limitations that hamper their wider deployment in devices. For example, although diamond and c-BN are known to conduct electricity upon doping by impurities, the activation energy of donors and acceptors is high, and only a small fraction of dopants are ionized at room temperature. The resulting high concentrations of non-ionized impurities strongly scatter free carriers and severely limit the carrier mobility at the doping levels needed for efficient devices. Moreover, although low-Al-content AlGaN alloys are used in applications such as high-electron-mobility transistors (HEMTs) and light-emitting diodes (LEDs), high-Al-content AlGaN is hampered by the increase in activation energy of acceptors with the increase in Al content and by the formation of donor

¹ Department of Materials Science and Engineering, University of Michigan, Ann Arbor, MI 48109, USA

²Applied Physics Program, University of Michigan, Ann Arbor, MI 48109, USA

³ Department of Electrical Engineering and Computer Science, University of Michigan, Ann Arbor, MI 48109, USA

a) Address all correspondence to this author. e-mail: kioup@umich.edu



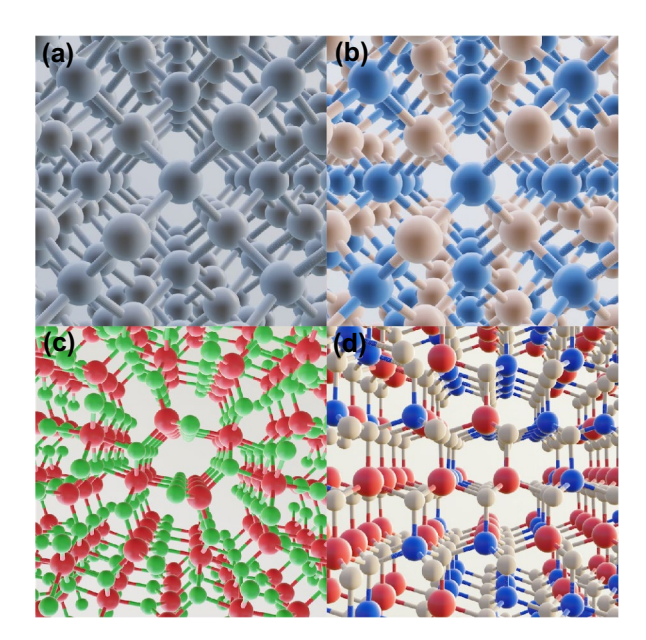


Figure 1: Crystal structure of the most actively researched UWBG semiconductors: (a) diamond, (b) cubic BN, (c) β -Ga₂O₃, and (d) AlGaN alloys.

DX centers that limit the free-electron concentration. Recently, β-Ga₂O₃ has attracted significant attention for power-electronics applications, primarily thanks to the feasibility of n-type doping, the relatively high electron mobility, and the availability of wide-diameter native substrates. Yet, the lack of p-type doping and its low intrinsic thermal conductivity pose fundamental limitations to the design of devices that can be realized based on Ga₂O₃.

Understanding the atomistic origin of these intrinsic materials limitations will guide engineering strategies to mitigate them and will help guide the design of new materials that surpass the current state of the art.

First-principles calculations based on density-functional theory (DFT) and related techniques are a predictive set of computational tools that can aid in the theoretical characterization of the fundamental properties of UWBG semiconductors. These quantum-mechanical computational methods have been validated across a wide range of materials systems. They provide atomistic and electronic insights into the chemical and physical properties of UWBG materials that complement experimental characterization and can probe properties that may be inaccessible to experimental techniques. Being inherently predictive in nature, these computational tools are able to move one step ahead of experiment and guide the discovery and design of new UWBG semiconductors with targeted properties for device applications.

In this work, we review first-principles computational methodologies based on DFT and related techniques that have been developed in recent years to understand and predict the structural and functional properties of UWBG semiconductors (Table 1). We first discuss computational methods that can theoretically characterize the synthesis, stability, and dopability of semiconducting materials. We then analyze methods that aim to understand their functional properties, such as the efficiency of charge and heat transport, their electrical behavior under high electric fields, and the efficiency of light emission. We conclude with a discussion on how high-throughput calculations and

TABLE 1: First-principles computational methodologies to characterize the properties of UWBG semiconductors, along with a summary of challenges and opportunities in each area.

Property	Methodology	Challenges and opportunities
Structure, thermodynamic stability, and synthesis	Total energy calculations, cluster-expansion methods	Accuracy, temperature effects, system scale, and complexity
Vibrations and thermal conductivity	Density-functional perturbation theory, frozen- phonon supercells, Boltzmann transport equation	Anharmonicity, treatment of different conduction regimes
Band gap, effective masses, valley energies, and band alignments	Band-structure calculations with many-body perturbation theory and/or hybrid functionals	Temperature effects, alloy disorder, and carrier localization
Defects and doping	Total energy with hybrid functionals	Accuracy of shallow dopant ionization energies, defect-defect interactions
Carrier mobility	Density-functional perturbation theory, Boltzmann transport equation	Accuracy of band structure, scattering by defects, alloy disorder, quantum transport
Polaron formation	Supercell calculations or perturbation theory	Accuracy, polaron transport
High-field transport and breakdown	Boltzmann transport equation with Monte- Carlo simulations	Non-equilibrium effects, quantum transport, system complexity
Optical properties and excitons	Bethe–Salpeter equation	Finite temperature, phonon screening, phonon-assisted optics
Carrier recombination	Calculations of Shockley–Read–Hall, radiative, and Auger recombination rates	Coulomb corrections at finite temperature and carrier concentration
Materials discovery	High-throughput calculations, materials informatics	Accuracy of high-throughput data, synergy of techniques



materials-informatics techniques can be leveraged to predict new candidate UWBG semiconductors that may surpass the current state of the art. In all cases, we highlight examples from the computational literature that demonstrate the successful applications of first-principles approaches to understand and predict the properties of UWBG semiconductors, and we discuss challenges and opportunities to advance the field.

Structure, stability, synthesis, and polarization

Materials-modeling techniques based on density-functional theory (DFT) have become an indispensable theoretical characterization toolkit that complements experimental studies, and they are widely applied to understand and predict the structural, mechanical, and thermodynamic properties of materials. The theoretical foundations of DFT have been extensively discussed in the literature, and we refer the interested reader to recent overviews for the technical details [4, 5]. The DFT methodology has been implemented in software such as Quantum ESPRESSO [6], ABINIT [7], and VASP [8]. With common approximations to the exchange-correlation functional, such as the local density approximation (LDA) [9, 10] or the Perdew-Burke-Ernzerhof (PBE) parameterization of generalized gradient approximation (GGA) [11], DFT calculations balance a high degree of predictive accuracy with a reasonable computational cost. The key quantity obtained from DFT is the total energy of the electrons and ions, which corresponds to the thermodynamic enthalpy of the material. In turn, the equilibrium coordinates of the atoms are calculated by varying the atomic positions until the total energy and the forces on the atoms are minimized. In the case of alloys that lack crystal periodicity, the total energy from DFT is fitted to cluster-expansion models (e.g., with the ATAT code [12]) and the configurational entropy is evaluated with statistical sampling by Monte-Carlo techniques. In recent years, hybrid exchange-correlation functionals that mix a fraction of exact exchange such as the range-separated Heyd-Scuseria-Ernzerhof (HSE) parameterization [13] have been shown to improve the quantitative agreement with experiment compared to LDA or GGA, including properties such as the magnitude of the band gap (see, e.g., the section on the Electronic Band Structure below).

DFT methods have been widely applied to uncover the structural, thermodynamic, and kinetic parameters of UWBG semiconductors. An illustrative example of thermodynamic calculations is the study of the enthalpy of mixing of Al_xGa_{1-x}N alloys [2], which identified alloy compositions that favor the formation of ordered compounds (Fig. 2a). Calculations along the same theme for (Al_xGa_{1-x})₂O₃ found that low-Al-content alloys adopt the monoclinic (β) phase and that Al preferentially substitutes the octahedral Ga sites [3]. Moreover, the calculations identified that the thermodynamically most stable phase at the equimolar composition is the ordered AlGaO3 compound (Fig. 2b). DFT calculations can also investigate kinetic processes in materials and shed light into the growth mechanisms, e.g., the work of Lymperakis and Neugebauer found that the diffusion barriers of Ga and N adatoms on non-polar GaN surfaces are anisotropic, and explain the growth anisotropy for these surfaces [14]. These results highlight the capabilities of DFT in understanding the stability and growth mechanisms of UWBG semiconductors.

The polarization properties of UWBG semiconductors can also be predictively described with DFT techniques. Materials that lack inversion symmetry can exhibit a finite electric dipole moment that gives rise to long-range electric fields and bound charges at their interfaces. These polarization fields are

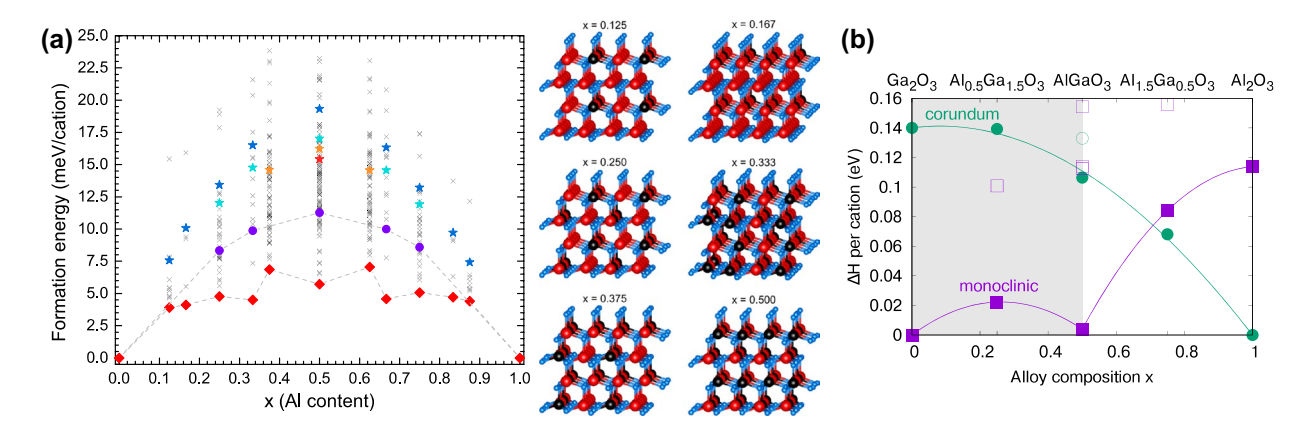


Figure 2: Examples of thermodynamic calculations with DFT applied to UWBG semiconducting alloys. (a) Mixing enthalpy of AlGaN alloys as a function of composition (left panel). The calculations identified alloy compositions that give rise to stable ordered structures (right panel). (b) Calculations for the mixing enthalpy of (Al,Ga) $_2$ O $_3$ alloys identified the stability of the ordered AlGaO $_3$ equimolar compound. Panel (a) reprinted with permission from Ref. [2], Copyright 2019, APS. Panel (b) reprinted with permission from Ref. [3], Copyright 2018, AIP Publishing.



an alternative way to realize free carriers without doping and create a two-dimensional electron (2DEG) or hole gas (2DHG) at, e.g., GaN/AlGaN interfaces. Calculations for the spontaneous polarization and piezoelectric constants of materials are based on the theory of King-Smith and Vanderbilt [15], and determine the polarization from the positions of the ions and the Berry phase of the valence-band manifold. Such calculations have been applied to understand the polarization constants of the group-III nitrides in order to resolve discrepancies in the reported empirical values [16]. Similar calculations for the polar epsilon phase of Ga₂O₃ (ε-Ga₂O₃) predicted the formation of a tunable 2DEG at its interfaces [17]. Further predictions include the formation of a 2DEG at the interface between GaN and ScN [18], due to the large polarization difference arising from the different crystal structures (wurtzite vs. rocksalt) of the two materials. The ability to assess the polarization of UWBG materials computationally is particularly important for device design, as it enables multiscale simulations of, e.g., carrier confinement in polar nitride quantum wells [19].

Despite these successful examples, DFT calculations still face challenges that limit their predictive power. One set of challenges revolves around the accuracy of DFT methods. Although the precision and reproducibility of modern DFT methods has been verified across different software implementations [20], there are no systematic recipes to improve the accuracy of DFT in comparison to experiment. In that front, functionals that account for the exact-exchange interaction, or that are constructed to satisfy exact constraints such as the Strongly Constrained and Appropriately Normed (SCAN) functional [21], are promising avenues to increase the DFT accuracy. Another challenge is the computational cost of DFT calculations for large and/or complex material systems that involve large numbers of atoms (on the order of several hundreds or more) such as alloys, surfaces, interfaces, and nanostructures. Advances in numerical implementations that harness the power of exascale machines are promising to enable DFT calculations for such computationally demanding problems.

Atomic vibrations and thermal conductivity.

Although atoms in crystalline semiconducting materials adopt, on average, a periodic structure in space, the instantaneous position of the atoms deviates from the perfect periodicity both due to thermal motion at finite temperature as well as due to zero-point motion by quantum-mechanical effects. These atomic vibrations (phonons) play an important role in the structural, thermodynamic, and functional properties of materials at finite temperature. For example, the Raman and infrared optical spectra, which arise from the interaction of photons with phonons, can be used to characterize the microstructure of a material sample, while the entropy due to thermal motion affects the

thermodynamic stability of materials at high temperature. Moreover, the interactions between electrons and the lattice vibrations scatter charge carriers and affect the mobility of materials (see, e.g., the section on the Low-Field Transport and Carrier Mobility below). Last but not least, the anharmonic interactions between phonons in a material pose a fundamental upper bound to its thermal conductivity, and thus to the efficiency of heat extraction from devices.

The properties of phonons in crystalline materials are investigated with density-functional perturbation theory [24], which can determine the phonon frequencies and atomic displacements for arbitrary phonon wave vectors solely from the primitive unit cell, including the long-range polar interactions [25]. Alternatively, the force constants between atoms can be determined as derivatives of the total energy with appropriately constructed supercells as in, e.g., Refs. [26] and [27]. Although the supercell methods can only study phonons with wave vectors commensurate with the size of the supercell, they have the advantage that can be combined with any functional that can supply the total energy (e.g., hybrid functionals). Both of these techniques can be extended to calculate anharmonic (third and higher order) interatomic force constants in materials, which are responsible for phonon-phonon scattering processes. The anharmonic force constants can be combined with the Boltzmann transport equation in software such as almaBTE [23] in order to determine the thermal conductivity of materials. A perspective on modern atomistic calculations for the thermal conductivity of ordered and disordered materials is presented in Ref. [28].

Atomistic phonon calculations have been instrumental in uncovering the fundamental vibrational properties of UWBG semiconductors. In recent years, these techniques have uncovered the full phonon dispersion of β-Ga₂O₃ (including the frequencies of the Raman- and infrared-active modes, Fig. 3a), and shed light into the directional anisotropy of its thermal conductivity and the important role of optical phonons in thermal transport in this material (Fig. 3b) [22, 23, 29]. Moreover, thermal-transport calculations in the ordered AlGaO₃ phase find that the thermal conductivity increases relatively to β-Ga₂O₃, primarily due to its reduced number of three-phonon scattering processes that satisfy energy and momentum conservation [30]. Calculations have also predicted that the thermal conductivity of c-BN increases by ~ 128% in isotopically pure samples [31] (subsequently revised to ~90% after the inclusion of four-phonon scattering [32]) due to the relatively high abundance of the ¹⁰B and ¹¹B stable isotopes, a prediction that was subsequently verified experimentally [32]. These examples demonstrate the predictive power of DFT in characterizing lattice vibrations and thermal transport in UWBG materials.

Although modern calculations offer unprecedented insights into the vibrational and thermal-transport



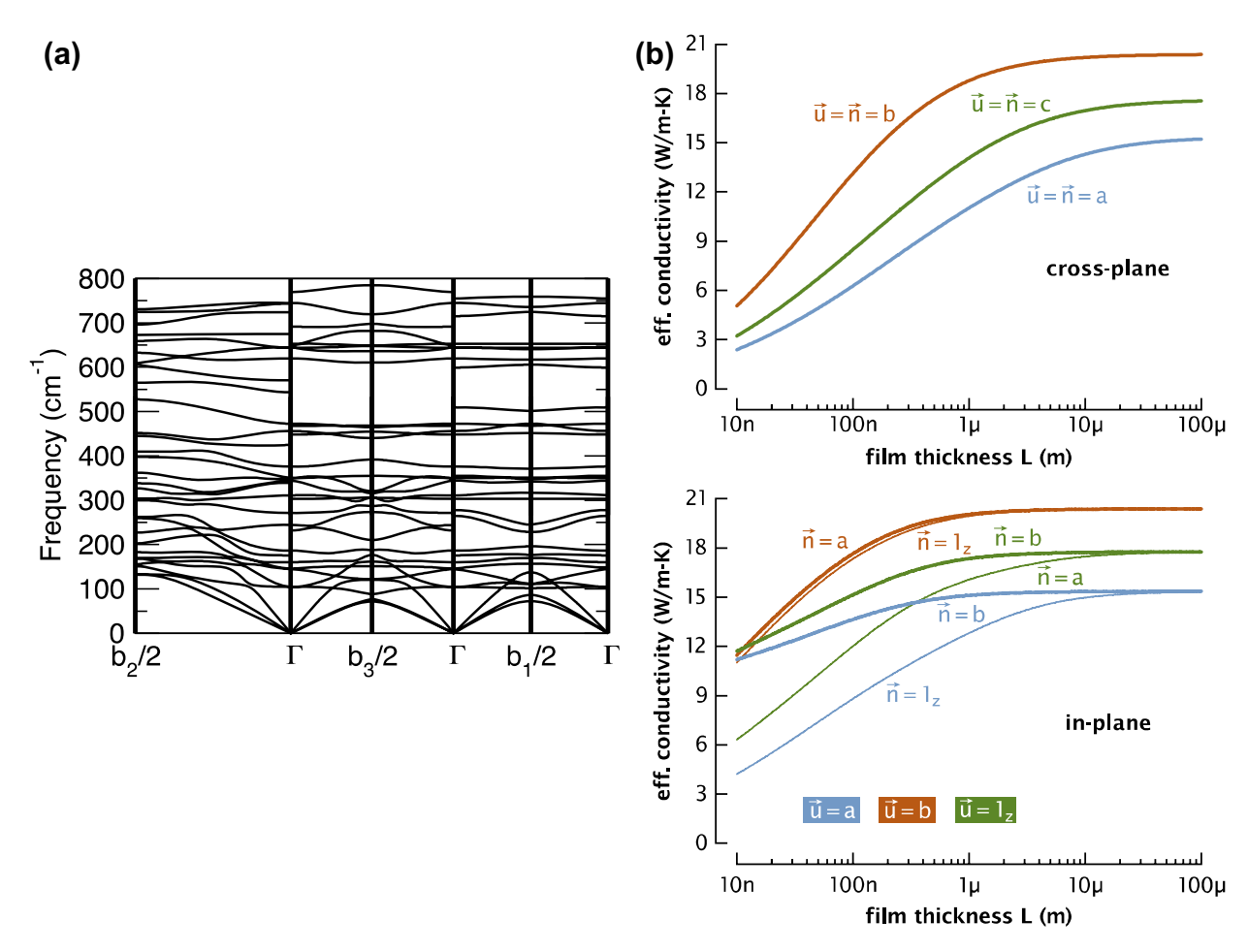


Figure 3: Examples of calculated vibrational properties of UWBG semiconductors. (a) The phonon dispersion of β-Ga₂O₃ identifies the frequencies of Raman-active and IR-active phonon modes. (b) The room-temperature anisotropic thermal conductivity of β-Ga₂O₃ as a function of film thickness. Panel (a) reprinted from Ref. [22]. Panel (b) reprinted with permission from Ref. [23], Copyright 2017, Elsevier.

properties, several challenges and opportunities remain. In addition to the challenges that stem from the accuracy and scalability of DFT, the treatment of anharmonicities remains an active research area. Anharmonicities have a strong effect on the frequencies of the vibrational modes in certain semiconductors (as in, e.g., PbTe [33]), while higher-order anharmonic effects (four-phonon scattering and beyond) play an important role in the thermal conductivity of numerous materials including diamond [34] and c-BN [32]. Another area is the treatment of disorder, particularly in alloys such as AlGaN [35] and in materials with high concentrations of point defects. A discussion of methods to treat disorder scattering is presented in Ref. [28]. Last but not least, the development of new methods that can describe thermal transport in crystals and in disordered materials in a unified fashion as in Ref. [36] offers new opportunities for the study of thermal transport in UWBG semiconductor alloys.

Electronic band structure

The electronic band structure of a semiconductor is a crucial material property that determines its functional properties. The existence of an energy gap between the highest occupied and the lowest unoccupied electronic states of a material not only dictates its fundamental electronic nature (metallic vs. semiconducting/insulating), but the magnitude of the gap also determines the strength of its intrinsic breakdown electric field [37]. In addition, the curvature of the bands near the band extrema controls the effective masses of free electrons and hence the electrical conductivity. Moreover, the existence of higher-energy features such as low-energy secondary valleys or inflection points affects carrier scattering at high fields and gives rise to oscillatory phenomena in device applications.

Despite the successes of density-functional theory in determining the structural, chemical, and vibrational properties



of materials, band-structure calculations that employ local approximations to the exchange-correlation functionals such as the LDA or the GGA severely underestimate the band gaps of semiconductors and insulators. The band-gap underestimation is typically on the order of 50%, but in extreme cases such as Ge or InN the gap closes entirely and thus DFT predicts them to be metals [38, 43]. Yet, over the past decades advances in electronic-structure theory have enabled the development of new methodologies that allow the determination of the band gaps of semiconductors and insulators with a typical accuracy of 0.1-0.2 eV. These include diagrammatic many-body perturbation theory (e.g., the GW method) [44], which applies quasiparticle corrections to the DFT band structure, or DFT calculations with hybrid exchange-correlation functionals such as the Heyd-Scuseria-Ernzerhof (HSE06) expression [13], which mix part of exact exchange to improve the description of the exchange-correlation energy. These two methods can also be combined by using the HSE wave functions and eigenenergies as a better starting point for GW calculations. An overview of these methods is presented in Refs. [45] and [46]. These techniques have been successfully applied to determine, e.g., the

band structures of the group-III nitrides, including consistent sets of band parameterizations (Fig. 4a) [38] and deformation potentials that account for the effects of strain [47]. The band gap of InN in particular, which is non-existent in LDA/GGA, is predicted to be in excellent agreement with the experiment once hybrid functionals [40] or GW corrections [38] are applied. GW calculations have also revealed how the crystalline anisotropy of $\beta\text{-}Ga_2O_3$ gives rise to a series of relatively flat valence bands that are close in energy (Fig. 4e), which in turn gives rise to different onsets of optical absorption in optical spectra and thus to a broad range of experimentally reported band-gap values (see section on Optical Properties and Excitons below) [39].

The absolute energies of the electronic bands are another set of important material parameters of semiconductors that determine their relative band alignment in heterostructures or at interfaces with metals and oxides. A common approach to evaluate the absolute band positions is the methodology of Van de Walle and Martin [48], which leverages the energy difference between the plane-averaged electrostatic potential of nonpolar slabs to determine the relative band positions between two materials or with respect to vacuum. Another method is

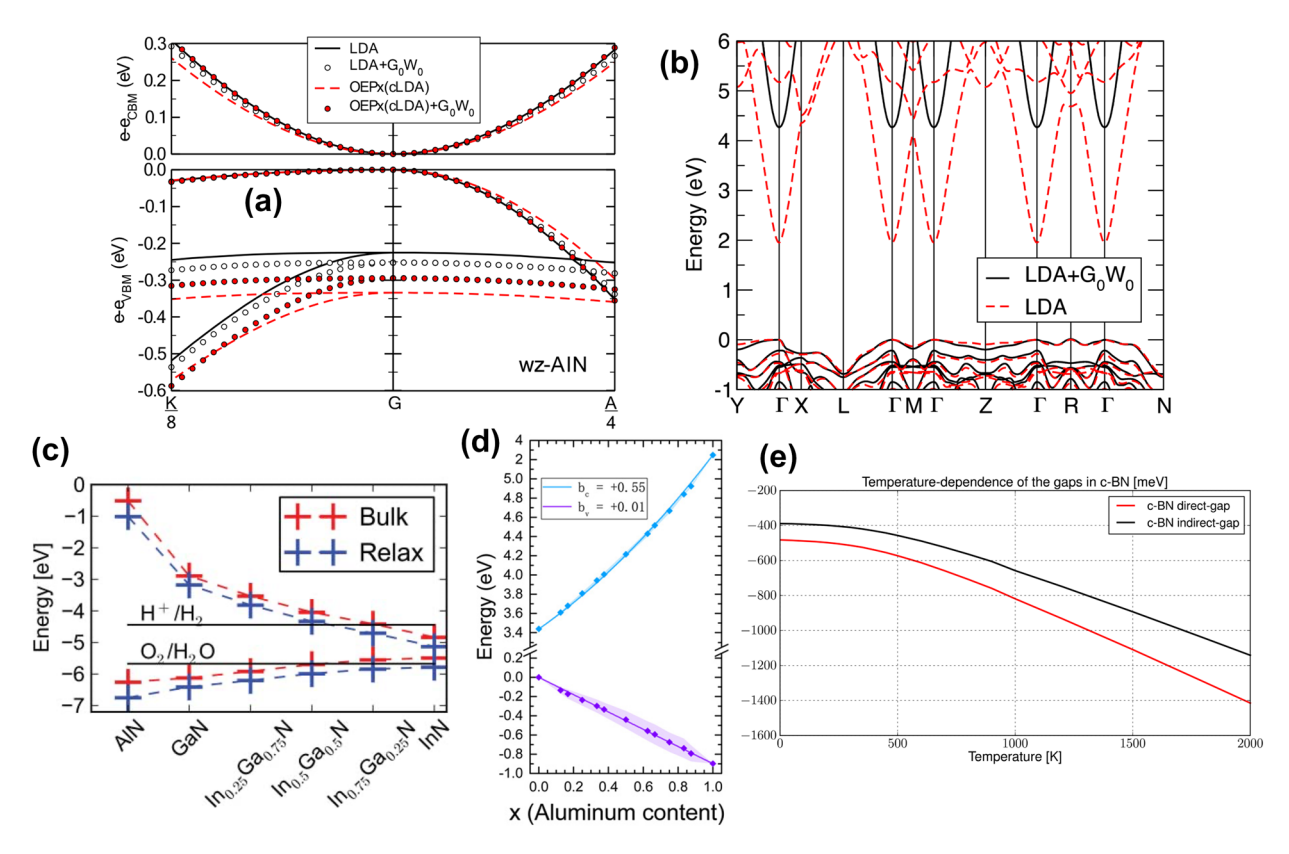


Figure 4: Examples of band-structure calculations for UWBG semiconductors. (a) Quasiparticle band structure of AlN. (b) Quasiparticle band structure of β -Ga₂O₃, demonstrating the flat valence and dispersive conduction band. (c) Band alignments of group-III nitrides calculated with the HSE functional. (d) Bowing of the valence and conduction bands of Al_xGa_{1-x}N calculated with HSE. ((e) Temperature dependence of the band gap of c-BN, including zero-point-motion corrections. Panel (a) reprinted from Ref. [38]. Panel (b) reprinted with permission from Ref. [39], Copyright 2016, AlP Publishing. Panel (c) reprinted with permission from Ref. [40], Copyright 2011, AlP Publishing. Panel (d) reprinted with permission from Ref. [41], Copyright 2020, IOP Publishing. Panel (e) reprinted with permission from Ref. [42], Copyright 2015, AlP Publishing.



based on the universal charge-transition level between the ± 1 and ± 1 charge states of interstitial hydrogen (see, e.g., section on Defects and Doping below) [49]. A third method employs the branch-point energies of the band structure as determined from the topmost valence and the lowest conduction bands. Such methods have been applied to determine the band alignment and band-gap bowing of AlGaN alloys as a function of alloy composition (Fig. 4b, c) [40, 41, 50].

Most band-structure calculations are performed at zero temperature, assuming the atoms are at rest in their equilibrium crystalline positions. However, real materials operate at finite temperature, at which lattice vibrations (see section on Atomic Vibrations and Thermal Conductivity above) affect their electronic properties. In addition, UWBG semiconducting materials contain light elements such as C, N, and O, that give rise to strong zero-point motion effects. Recent theoretical developments in the study of electron-phonon interactions have enabled the study of zero-point motion and finite-temperature effects on the electronic band structure of UWBG semiconductors, e.g., Giustino et al. calculated the effects of electron-phonon interactions on the direct band gap of diamond as a function of temperature, and found that zero-point motion reduces the gap by as much as 0.6 eV [51]. Other calculations found that zero-point motion and finite-temperature effects reduce the band gaps of several UWBG semiconductors such as AlN, diamond, and c-BN by several hundreds of meVs [27, 42]. These results point to the important role of electron–phonon coupling corrections on the electronic properties of UWBG semiconductors.

In spite of recent breakthroughs, several challenges remain open to enable accurate band-structure calculations in UWBG semiconductors at room temperature. Although finite-temperature corrections to the band structure by electron-phonon interactions have now been established, they are far from routine and have only been performed for a few materials and/or for specific high-symmetry points of the Brillouin zone. The development of new methodologies that enable calculations of the temperature dependence of the entire band structure, such as the fully anharmonic non-perturbative theory of Zacharias et al. [52], will help shed light not just on the temperature evolution of the band gap, but also on the variation of crucial material parameters such as effective masses, band velocities, and valley energies at finite temperature. Moreover, the computational cost of accurate band-structure calculations with hybrid functionals or many-body perturbation theory makes them prohibitively expensive for the large supercells needed to accurately capture long-range alloy disorder. To enable electronic-structure calculations that capture the effects of carrier localization by composition fluctuations in alloys, further advances in the seamless integration of multiscale techniques that combine accurate band parameters from hybrid DFT or many-body perturbation theory with the scalability of methods such as $k \cdot p$ or tight binding [53] are necessary.

Defects and doping

A defining feature of semiconductors is the presence of mobile free carriers provided by the ionization of intentional dopants or unintentional defects that enable the conduction of electricity. However, in semiconductors with ultra-wide band gaps, achieving the desired polarity or level of doping becomes challenging if not outright impossible. As the UWBG semiconductors have relatively small lattice constants, there is a limited number of dopants that can fit into the lattice without inducing too much strain. Also, as the UWBG semiconductors have a low-lying valence-band maximum or a high-lying conduction-band minimum relative to the vacuum level, even the optimal substitutional dopants may have activation energies significantly exceeding the thermal energy at room temperature, preventing their efficient thermal ionization. In addition, charge-compensating native defects or impurities are easier to form and consume the free carriers. For example, dopant ionization energies of known substitutional dopants in c-BN, AlN, and diamond range in the order of a few 100 meV (e.g., 0.24 eV for acceptors in c-BN [57]), which significantly limits their doping efficiency. Such high ionization energies also occur for Mg acceptors in GaN, and lead to high concentrations of non-ionized acceptors that, among other things, cause strong internal absorption loss in (In)GaN lasers [58]. Yet, many point-defect properties are challenging to characterize experimentally, since defect-related phenomena occur at the length scale of individual atoms and defect concentrations are often dilute (on the order of parts per million). For that purpose, modern point-defect calculations have evolved into a powerful theoretical characterization framework that can predict the formation and ionization energy of native point defects, intentional dopants, and unintentional impurities in order to uncover the efficiency of and limitations to the doping of UWBG semiconductors.

An overview of the modern methodology for point-defect calculations based on hybrid density-functional theory is presented in review articles by Van de Walle and co-workers [59]. The methodology evaluates the formation energy of point defects as total-energy differences between supercells that contain the investigated defects in the targeted charge state and the pristine semiconductor, as well as the total energies of reference states and any secondary phases. Additional methodologies correct the artificial interactions between periodic images of charged defects [60]. The resulting formation energies determine the stable defect charge states as a function of growth conditions (e.g., cation-rich or cation-poor growth) and Fermi-level position (e.g., under n-type or p-type doping), and can identify charge-transition levels and dopant ionization energies. The



methodology can also identify potential charge-compensating defects that compete with the formation of shallow dopants and potentially pin the Fermi energy far from the band edges. The solubility of dopants under the experimental growth conditions can also be obtained from their formation energy via an Arrhenius equation. Finally, the equilibrium Fermi level and free-carrier concentrations can be evaluated self-consistently using as input the charged-defect formation energies and the densities of states of the conduction and valence bands.

Defect calculations have provided valuable insights into the doping properties of UWBG semiconductors. For example, calculations for dopants and defects in Al, Ga1-, N alloys shed light on the efficiency of n-type and p-type doping, as well as its dependence on alloy composition, e.g., defects that act as shallow donors in Ga-rich AlGaN such as Si, Ge, and O become self-compensating DX centers at high Al concentrations. Calculations have revealed that Si is the most effective among these three donors in Al-rich AlGaN, as the formation of Si DX centers pins the Fermi level at a higher energy (up to ~ 150 meV below the conduction-band minimum of AlN, Fig. 5a) [54]. With regard to p-type doping, substitutional group-II elements such as Mg and Be have been shown to act as acceptors in AlN [61]. However, the acceptor ionization energies are high (~0.8 eV) [62] and they are compensated by N vacancies [63]. Yet, calculations have also revealed that the doping efficiency can be improved through Fermi-level engineering, either by growing the material in the presence of UV illumination with photon energies above the band gap [64, 65] or by the formation of a

metal–semiconductor junction during molecular beam epitaxy [55]. Both these techniques shift the Fermi level farther from the valence-band edge, therefore simultaneously decreasing the acceptor formation energy and increasing the energy cost for the formation of compensating N vacancies (Fig. 5b). The efficiency of p-type doping can also be improved by growing Al-rich AlGaN under N-rich conditions, which also promote the incorporation of acceptors while reducing the concentration of N vacancies (Fig. 5c) [56]. Similar results have also been obtained for dopants in BN polytypes, in which group-II elements have also been predicted to be good candidate acceptors (Fig. 5d) [57].

The success of point-defect calculations in UWBG semiconductor research stimulates further methodological developments to advance the state of the art in the field. For example, although the accuracy of point-defect formation energies is sufficient to discern the occurrence of specific defects species, it is not high enough to enable accurate predictions of defect concentrations or diffusion coefficients. This is because both of these quantities are exponentially dependent on the formation energy and the migration barrier, respectively, and are thus sensitive to the intrinsic accuracy of DFT calculations. Moreover, accurate calculations for the ionization energies of shallow dopants require large supercells (on the order of several nanometers wide) to prevent the overlap of their delocalized wave functions, which are intractable using hybrid functionals on modern computers. In this respect, a recently developed tandem approach that combines hybrid DFT with the long-range potential from

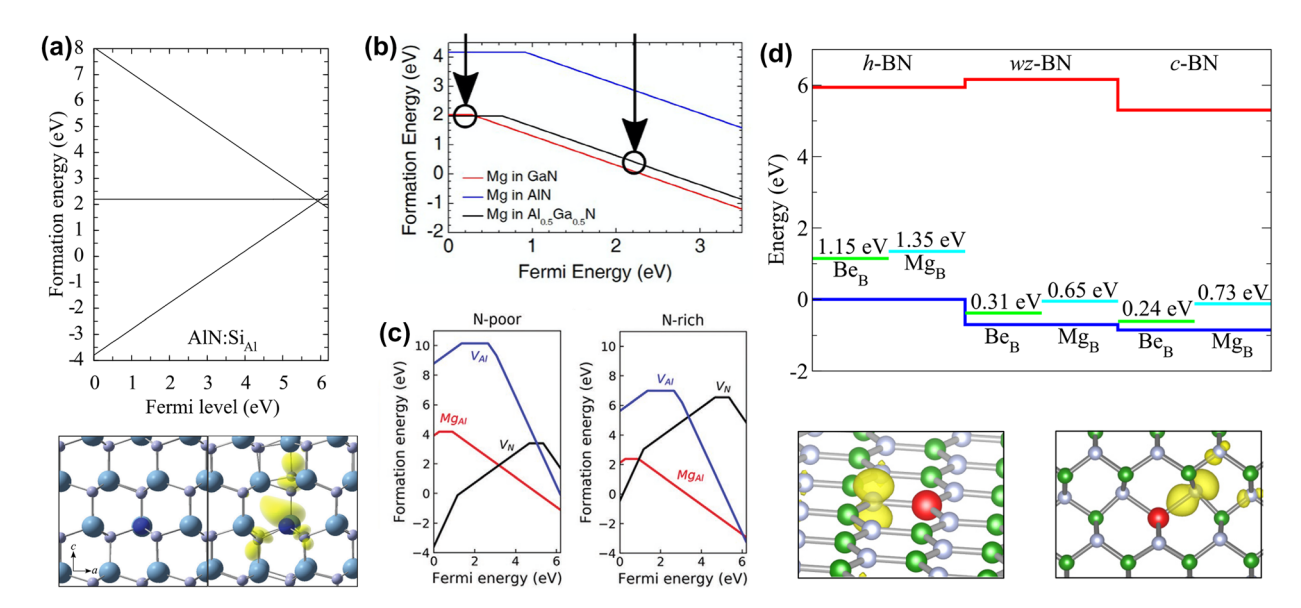


Figure 5: Highlights of predictive calculations for point defects and dopants in UWBG nitrides. (a) DX center formation by substitutional Si in AIN. Si is the most effective donor in AIN and AI-rich AIGaN alloys. (b, c) The formation energy and concentration of Mg acceptors in AIN and AIGaN, and thus the efficiency of p-type doping, can be controlled by (b) engineering the Fermi level through, e.g., junction-assisted epitaxy, or (c) growth under N-rich conditions. (d) Substitutional Be is a relatively shallow acceptor in wurtzite and zincblende BN. Panel (a) reprinted with permission from Ref. [54], Copyright 2014, APS. Panel (b) reprinted with permission from Ref. [55], Copyright 2019, APS. Panel (d) adapted with permission from Ref. [57], Copyright 2017, APS.



GGA has produced accurate results for shallow donors in silicon [66] and can be generalized to study shallow dopants in UWBG semiconductors as well. On the other hand, the modern methodology of point-defect calculations focuses on the dilute defect-concentration limit and neglects defect-defect interactions that modify the defect energetics. Therefore, obtaining accurate ionization energies as a function of doping concentration is challenging for shallow dopants (for which the long exponential tails of their delocalized wave functions overlap and give rise to impurity bands) or for heavily doped materials (in which neighboring defects interact and modify the band structure of the host). Therefore, methodological developments for the systematic treatment of defect-defect interactions provide a fruitful ground of research opportunities.

Low-field transport and carrier mobility

The carrier mobility is a crucial parameter to describe low-field electronic transport in semiconductors, as it determines the heat generated by Ohmic losses and controls the efficiency of devices. Calculations of the carrier mobility require an accurate description of the electronic band structure in combination with the evaluation of carrier scattering by phonons and impurities. Historically, these calculations are performed using empirical models based on, e.g., k·p, tight-binding, and/or deformation potential theory that fit the key semiconductor parameters (such as the band gap, valley energies, effective masses, and deformation potentials) to available experimental data. However, the range of validity of these band-structure and scattering models is limited, while calculations that rely on empirical parameters cannot provide mobility values that are independent of experiment or predictive for new materials. These shortcomings require ab initio methods that can not only predictively calculate carrier mobilities in a parameter-free way, but also provide a tool for characterizing the underlying mechanisms that affect this important material property.

Recent advances in first-principles methods and code development aim to understand the mechanisms that limit the carrier mobility in UWBG semiconductors as a function of chemical composition, temperature, doping, and strain, as well as to enable the prediction of new materials with improved transport properties compared to the current state of the art. To enable predictive calculations of carrier mobilities, accurate band structures from many-body perturbation theory or hybrid-functional DFT (see, e.g., section on the Electronic Band Structure above) are combined with the first-principles evaluations of the electron-scattering probability rates from phonons, defects, and alloy disorder to iteratively solve the Boltzmann transport equation for carriers and determine their steady-state distribution over energy states [71]. A significant numerical challenge in evaluating the carrier mobility lies in the fact that free

carriers in semiconductors often occupy only a small fraction of the first Brillouin zone, and their scattering probabilities over initial and final states need to be evaluated on fine sampling meshes. Although performing a single electron-phonon scattering calculation for the matrix element between a specific pair of initial and final states is routine, performing the brute-force sum over all possible combinations of initial and final states becomes numerically intractable even on the largest available supercomputers. A recent development that has drastically accelerated calculations of materials properties mediated by electron-phonon coupling is the efficient interpolation of the band structure, phonon energies, and, most importantly, the electron-phonon coupling matrix elements using maximally localized Wannier functions [72] that has been implemented to iteratively solve the Boltzmann transport equation in codes such as EPW [73] and PERTURBO [74], among others. This method even enables the interpolation of non-analytical contributions such as the Fröhlich [25] and quadrupole [75, 76] corrections. We direct the reader to Ref. [77] for an in-depth review of the phonon-limited mobility and conductivity calculations in bulk and 2D semiconductors. In parallel, computational methods based on supercells have been developed in order to quantify scattering by defects [78, 79] and alloy composition fluctuations [80], and to evaluate the carrier mobility in disordered materials.

These developments in first-principles calculations have enabled numerous computational studies that elucidate and predict the transport properties of UWBG semiconductors. In one example, Poncé et al. evaluated the phonon-limited carrier mobilities in GaN (Fig. 6a) [67, 81]. They demonstrated that by reversing the sign of the crystal-field splitting of the valence bands via bi-axial strain, the hole mobility increases by up to 230% due to the reduction of the density of final states available for hole scattering. In the case of β-Ga₂O₃, theoretical calculations reproduce the experimentally measured material properties and provide additional insights into the factors that limit the carrier mobility. In contrast to zincblende or wurtzite semiconductors, calculations show that the low-frequency polar-optical phonon modes induced by the low-symmetry of the β-Ga₂O₃ structure are thermally active at room temperature and have a strong effect on suppressing its electron mobility (Fig. 6b) [22, 68, 82, 83]. Further expanding the first-principles toolbox, Pant et al. developed a computational method to determine the electron-scattering rates due to alloy disorder by unfolding the DFT band structure from the alloy supercell to the primitive cell [69]. They evaluated the alloy-scattering-limited mobility of Al_xGa_{1-x}N alloys across the entire composition range, and found that even the lowest value of 186 cm²/Vs is comparable to the highest mobility expected in the related $(Al_rGa_{1-r})_2O_3$ system (Fig. 6c). In another example, by evaluating contributions to carrier scattering by phonons, ionized impurities, and neutral defects in diamond and c-BN, Sanders and Kioupakis



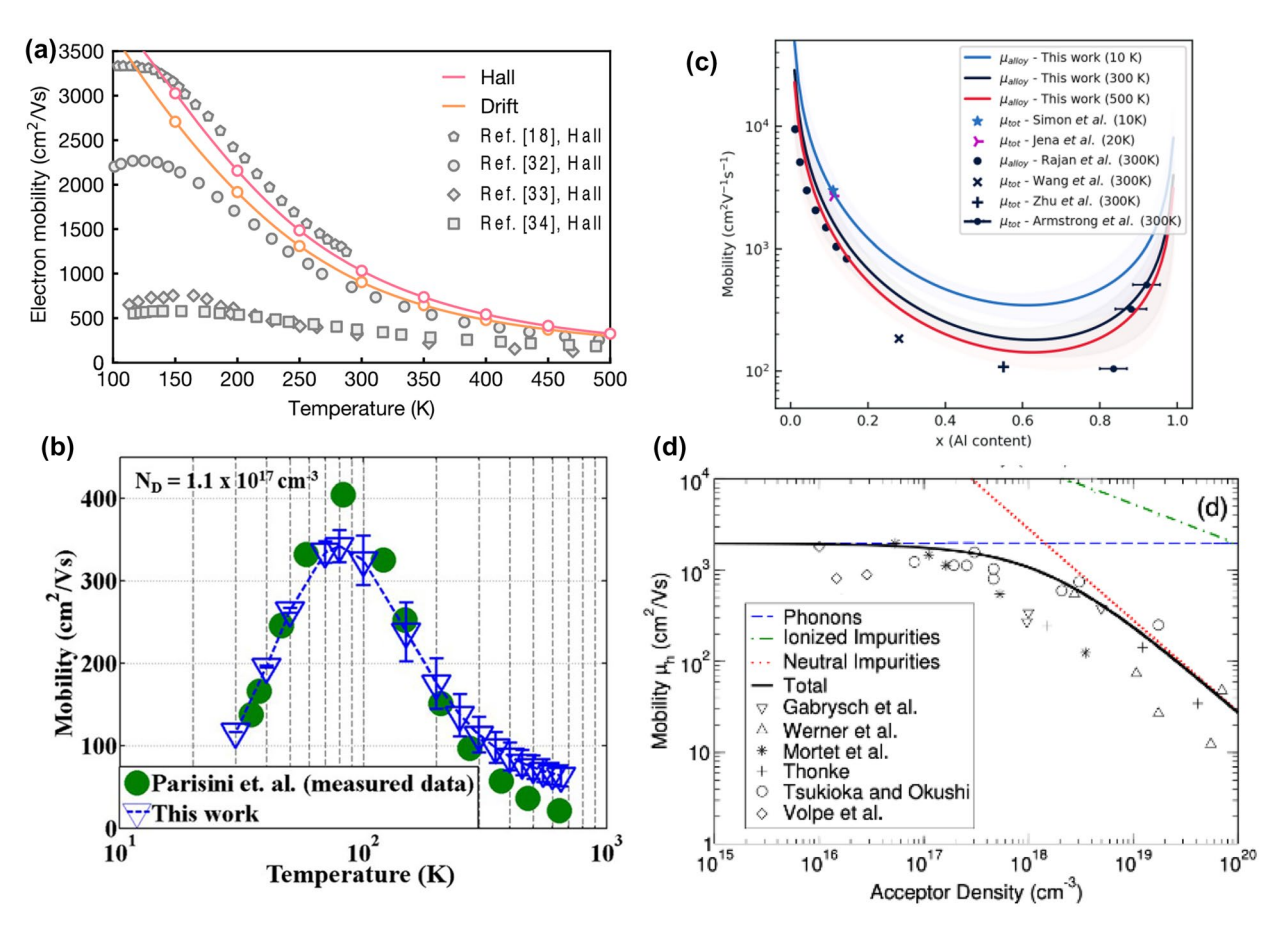


Figure 6: Theoretical results for the low-field carrier mobility of ultra-wide-band-gap semiconductors. (a) Phonon-limited electron mobility of GaN as a function of temperature. (b) Electron mobility of β-Ga₂O₃ as a function of temperature considering electron–phonon and ionized-impurity scattering. (c) Alloy-scattering contribution to the room-temperature mobility of AlGaN alloys as a function of composition. (d) Room-temperature hole mobility of diamond as a function of acceptor concentration, including electron–phonon, ionized-impurity, and neutral-impurity scattering. Panel (a) reprinted with permission from Ref. [67], Copyright 2019, APS. Panel (b) adapted reprinted with permission from Ref. [68], Copyright 2016, AlP Publishing. Panel (c) reprinted with permission from Ref. [70], Copyright 2021, AlP Publishing.

demonstrated that neutral defects are an important source of carrier scattering in these UWBG materials [70]. This is because the high ionization energy of donors and acceptors in c-BN and diamond require high dopant concentrations to realize sizable conductivities, and as a byproduct they introduce high concentrations of non-ionized impurities that act as carrier scatterers (Fig. 6d). This array of results highlights the breadth of insights that first-principles calculations can provide into the transport properties of UWBG materials.

While first-principles mobility calculations have demonstrated numerous successes, there are still many challenges to overcome and opportunities for further development. One challenge is improving the accuracy of the predicted mobility values, as they are sensitive to the calculated DFT material parameters such as the carrier effective masses. In practice, phonon-limited mobility values can vary widely even for materials as simple as silicon, depending on the DFT approximations used [73], and require a number of higher-order physically motivated

corrections to the DFT properties (e.g., quasiparticle corrections, spin-orbit coupling, corrections to the screening, and electron phonon renormalization) to reach predictive accuracy. With regard to defect-limited mobility calculations, emerging challenges are the inclusion of long-range Coulomb scattering by defects [79] and the treatment of inelastic scattering, e.g., charge trapping effects [84]. Moreover, DFT calculations of alloy disorder require an accurate description of local atomic ordering as in, e.g., (Al_xGa_{1-x})₂O₃, and need to be performed for large supercells in order to capture long-range carrier scattering and localization. While analytical models can be fit to DFT data to describe intra-band carrier scattering [69], extensions are needed to describe multiband scattering and transport. Moreover, the transport of localized carriers in alloys needs a description of the electronic states and electron-phonon interactions in disordered systems to describe hopping between localization sites [85]. The scale of DFT calculations can be extended to describe alloys by combining with model Hamiltonians such



as, e.g., atomistic tight binding [53] at the cost of limiting the predictive accuracy. Finally, further development in the unified description of semiclassical and quantum transport is needed to describe transport in nanoscale devices, in which ballistic effects become important [86].

Polarons

A challenge with the electronic conduction properties of certain UWBG materials is that carriers tend to form self-trapped polarons. The formation of a polaron stems from the electron–phonon interaction primarily in polar materials and results in the spatial localization of the carrier wave functions that is accompanied by a localized distortion of the crystal lattice (Fig. 7a). Polarons tend to bind more strongly in highly polar materials (as quantified by a large difference between the static and the high-frequency dielectric constants) and in materials with heavy carrier effective masses (since the spatial localization

of a heavier carrier results in a lower kinetic-energy penalty). These conditions are more likely to be met in materials with ultra-wide band gaps, as the carrier effective masses increase with the increase in band gap and because a larger electronegativity difference between the constituent elements results both in a stronger bond polarity and in a wider band gap. Also, polaron formation is more likely to occur for holes as they tend to have heavier effective masses than electrons in ultra-wide gap materials. In the weak-coupling regime (large Fröhlich polarons), the motion of polarons resembles that of free carriers, albeit with an increased effective mass. In the strong-coupling regime (small Holstein polarons), the carriers are localized at the atomic scale and transport by thermally activated hopping between localized sites. In both cases, polaron formation is detrimental to the carrier mobility compared to free carriers.

The theory of polarons and computational approaches to polaron properties were recently reviewed by Franchini and co-workers [87]. In the most direct computational approach,

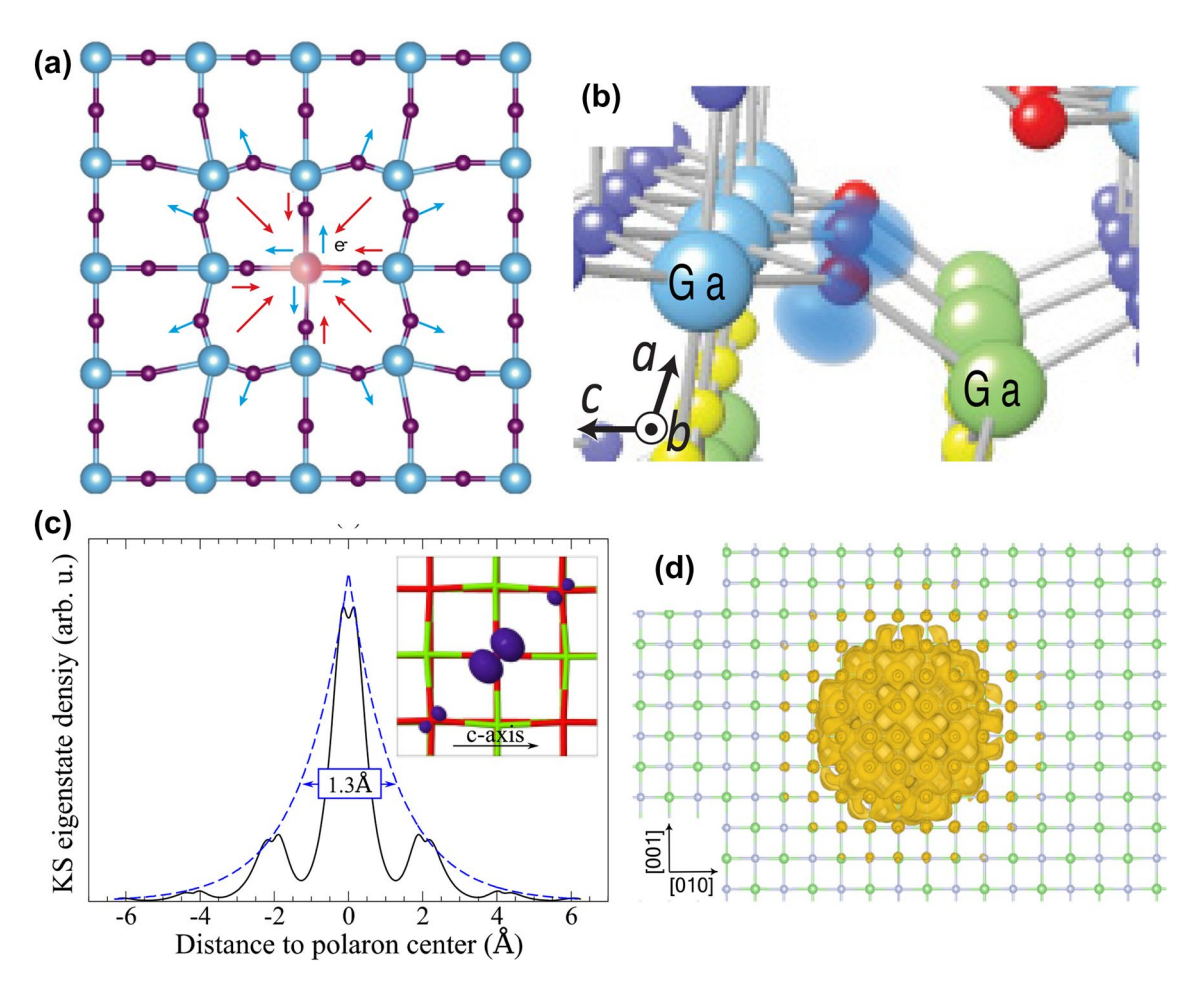


Figure 7: Highlights of polaron calculations in UWBG materials. (a) Schematic view of the formation of a self-trapped electron polaron. (b) A self-trapped hole polaron in β -Ga₂O₃. (c) Hole polarons in MgO. (d) A large polaron in LiF calculated without supercells. Panel (a) reprinted with permission from Ref. [87], Copyright 2021, Springer Nature. Panel (b) reprinted with permission from Ref. [88], Copyright 2012, APS. Panel (c) reprinted from Ref. [89]. Panel (d) reprinted with permission from Ref. [90], Copyright 2019, APS.



polarons are studied by adding an extra carrier (electron or hole) into a DFT simulation supercell and allowing the atoms to relax in the presence of the extra carrier [89]. The resulting atomic distortions create an attractive potential that localized the extra carrier. The supercell approach works best for strongly localized polarons, such that the polaron radius is smaller than the size of the supercell (i.e., on the order of 1 nm) to avoid artificial polaron-polaron interactions arising from the periodicity of the supercell. Moreover, these calculations are usually performed with hybrid functionals in order to obtain a more accurate description of exchange and correlation effects. Such calculations have been applied to uncover the strongly localized nature of hole polarons in UWBG oxides such as β-Ga₂O₃ [88, 91] (Fig. 7b) and MgO [89] (Fig. 7c). Large polarons, on the other hand, are computationally more challenging to capture with the supercell approach, as artificial interactions between periodic images affect the polaron energies and wave functions. In these situations, a computationally efficient approach relies on expanding the localized carrier wave functions and accompanying lattice distortions onto the basis of the pristine crystal Bloch functions and phonons, respectively [90, 92]. By iteratively solving the polaron equations, one can derive the polaron energies and wave functions without the use of supercells (Fig. 7d).

Despite the successes mentioned above, the quantitative description of polarons from first principles is a recent development, and several challenges remain open. Calculations so far have focused primarily on the formation and stability of polarons, while their transport properties remain less explored. Further advances that simultaneously describe both the hopping of bound polarons and the diffusive transport of thermally dissociated free carriers would be necessary to describe transport in materials that host polarons.

High-field transport and dielectric breakdown

The main advantage of ultra-wide-band-gap semiconductors for electronic devices is that their higher breakdown electric fields allow them to operate at much higher applied electric fields than their narrower-gap counterparts. At such high fields, the carrier drift velocity is not proportional to the applied field, and electronic transport is better described by the non-linear velocity-field curves. Moreover, the steady-state distribution of carriers under high fields deviates far from equilibrium, and carriers are accelerated to energies that can reach the order of eV. At these high energies, the bands show strong deviations from simple models such as the parabolic-band approximation or k-p parameterizations. It is thus vital to calculate band structures that accurately describe the energy dispersion of these highly excited carriers. Moreover, if the energies of these carriers with respect to the band minimum exceeds the band gap, they

can initiate impact-ionization processes that lead to avalanche breakdown and the failure of the device. It is thus crucial for device design to understand the atomistic origin of the fundamental limitations to high-field carrier transport in ultra-wideband-gap semiconductors.

A quantitative description of high-field transport requires an accurate description of the electronic band structure for energies up to several electron-volts away the band extrema. Such states have wave vectors that may span the entire width of the Brillouin zone and may involve multiple electronic bands. To describe these states, the band structure can evaluated accurately with many-body perturbation theory and/or hybrid functionals, and subsequently interpolated throughout the Brillouin zone with the maximally localized Wannier function method [95]. The matrix elements for carrier scattering by phonons can be evaluated with density-functional perturbation theory and also interpolated using Wannier functions (e.g., with the EPW code [96]). Such calculations have been applied to uncover the velocity-field curves and carrier distributions in ultra-wide-band-gap semiconductors such as AlGaN [93] (Fig. 8a) and β-Ga₂O₃ [94] (Fig. 8b). Impact ionization can be studied by combining the band structure with the Coulomb-scattering matrix elements. Kotani and van Schilfgaarde evaluated the impact-ionization rate using the imaginary part of the GW self energy for a series of semiconductors that includes GaN [97], while Ghosh and Singisetti performed a full-band Monte-Carlo simulation to investigate impact ionization in β-Ga₂O₃ [98]. The breakdown electric field can also be determined from first principles by comparing the rate of energy gain from the electric field to that of energy loss to the phonons [99], a technique that has been applied to determine the breakdown electric field of β-Ga₂O₃ as a function of temperature (Fig. 8c) [83]

First-principles calculations of high-field transport are at their early stages, and further methodological advances are necessary in order to enable accurate materials characterization and device design, e.g., carrier transport under high electric fields gives rise to out-of-equilibrium dynamics of carriers and phonons, and requires the simultaneous description of ultrafast hot-electron and hot-phonon effects as in Ref. [100]. Moreover, ballistic-transport phenomena may become relevant in nanometer-thin devices, and further methodological developments that account for quantum-transport effects may be necessary to describe device behavior at such short length scales.

Optical properties and excitons

The response of UWBG semiconductors to optical excitation provides valuable characterization insights into their material properties and facilitates the design of their optoelectronic devices. Recent developments in both theoretical methodologies and computational frameworks have enabled the accurate and



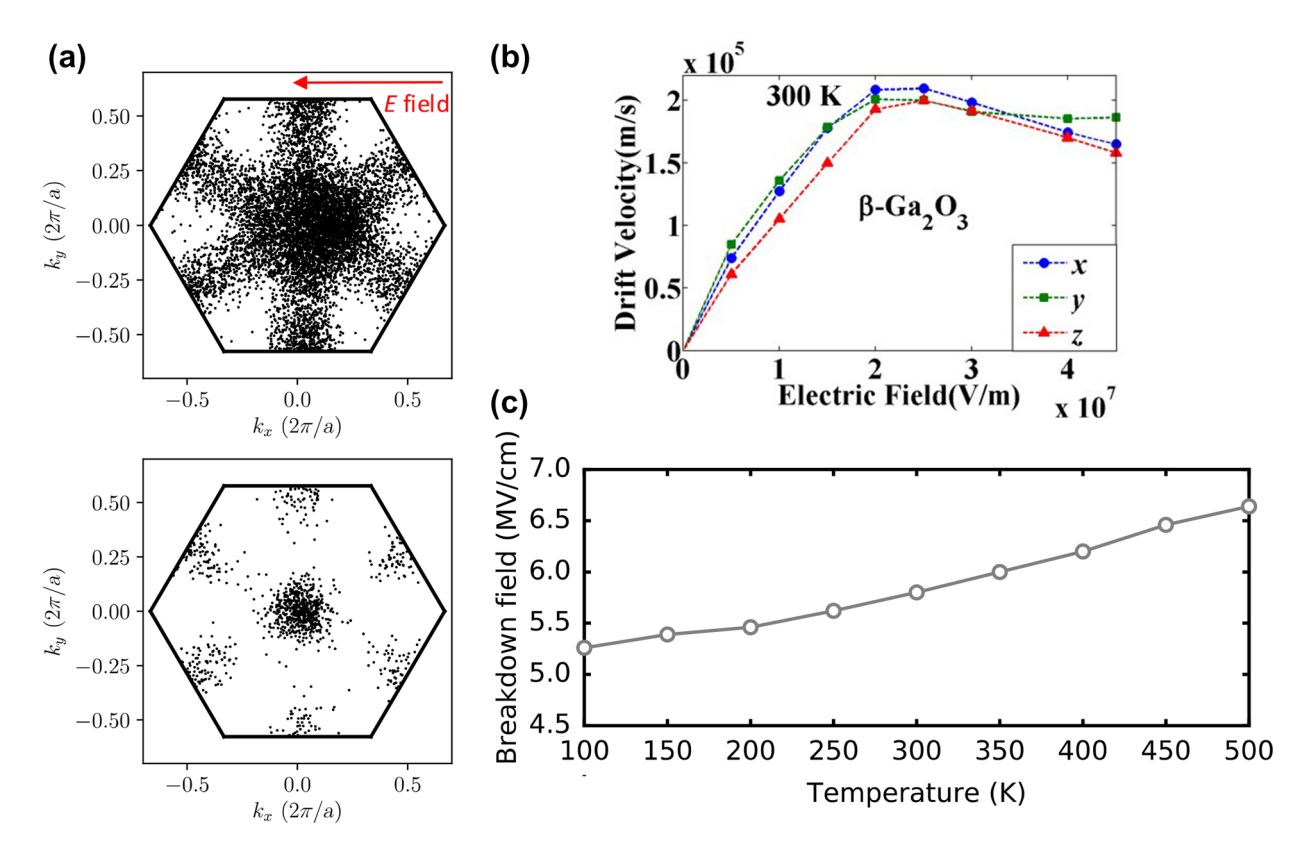


Figure 8: Examples high-field transport calculations with DFT. (a) Distribution of electrons over the first Brillouin zone of GaN for the first (top) and second (bottom) conduction band for an applied electric field of 800 kV/cm. (b) Velocity–field curves in β-Ga₂O₃. (c) The breakdown field of β-Ga₂O₃ as a function of temperature. Panel (a) reprinted with permission from Ref. [93], Copyright 2019, APS. Panel (b) reprinted with permission from Ref. [94], Copyright 2017, AIP Publishing. Panel (c) reprinted from Ref. [83].

detailed investigation of the optical and excitonic properties of UWBG materials. A review of predictive frameworks based on DFT and many-body perturbation theory to calculate the optical properties of materials is presented in Ref. [101]. Optical calculations start with the quasiparticle band structure and employ Fermi's golden rule to evaluate the complex dielectric function, accounting for all possible optical transitions between occupied and empty electronic states. Due to the Coulomb interaction between photoexcited electrons and the generated holes in the valence band, accurate simulations of optical properties need to account for the modification of the optical transition energies and probabilities due to the formation of excitons, i.e., bound electron-hole states, within the framework of the Bethe-Salpeter equation (BSE) formalism [102]. Continuous improvements in linear-algebra packages and numerical algorithms have resulted in the development of highly efficient parallel codes such as BerkeleyGW [44], Yambo [103], and Jena-BSE/ChASE [104], that enable optical/excitonic calculations for simulation cells containing hundreds of atoms.

First-principles computational methods have provided insightful connections between the optical properties of UWBG materials and their underlying atomic and electronic structure. Calculations for the near-edge optical absorption spectrum of

β-Ga₂O₃ demonstrated that its absorption onset is directionally anisotropic and dependent on the relative orientation of the optical polarization with respect to the crystal axes, which explains the origin behind the relatively broad range of experimentally reported band-gap values measured by optical techniques (Fig. 9a) [39]. In addition, calculations for the optical spectra of In₂O₃ and Ga₂O₃ found that excitonic corrections are necessary to obtain good agreement with experimental measurements (Fig. 9b) [105]. Moreover, optical calculations for metastable ZnO phases demonstrate that the measured optical spectra can be applied as a materials characterization tool to identify the underlying structural polytype in thin-film samples [109]. These examples demonstrate that accurate calculations of the optical properties of UWBG semiconductors provide a valuable theoretical characterization tool and can predict the optical response of candidate materials for device applications.

Many-body calculations with the BSE method are applied not only to study optical spectra, but also to understand the exciton properties of materials that are important in carrier recombination (see section on Radiative and Non-Radiative Recombination below). The exciton binding energy in most bulk semiconductors is low (e.g., on the order of 10 meV for the III-V family), which implies that excitons are thermally



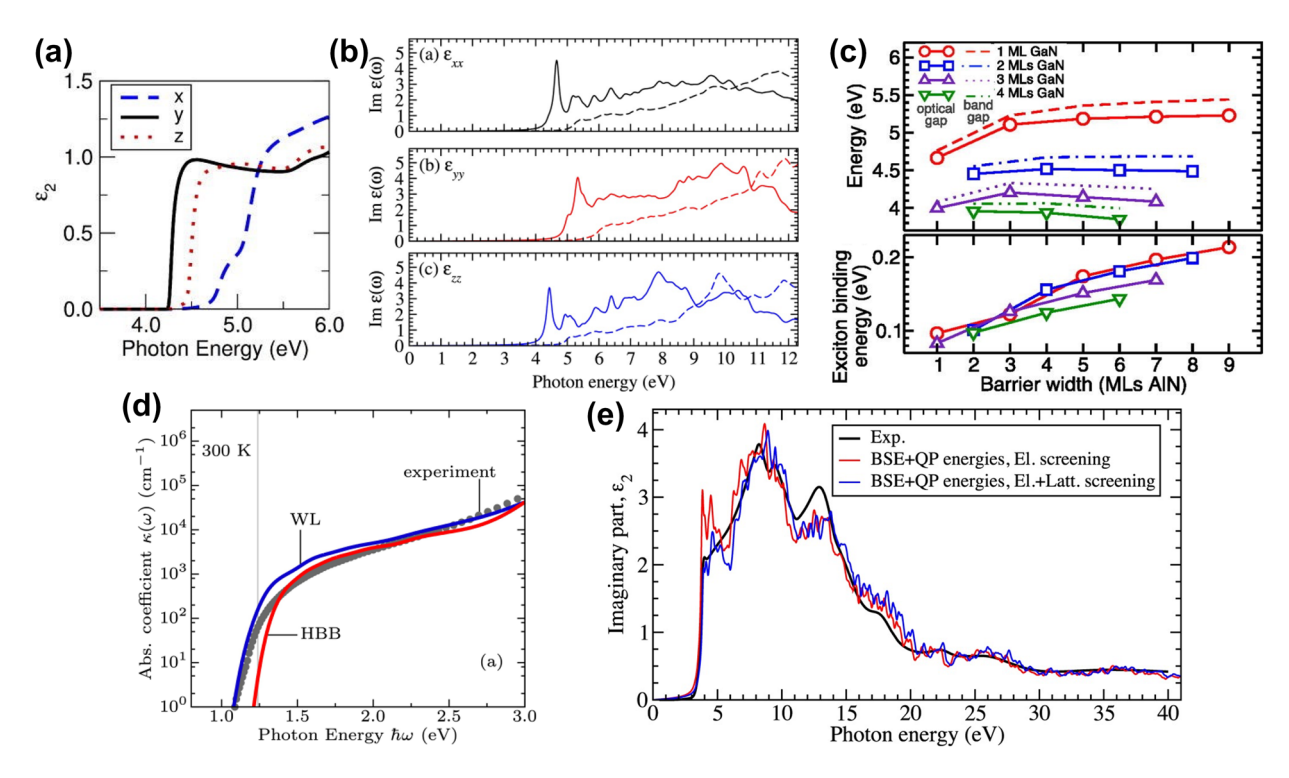


Figure 9: An overview of optical and excitonic calculations in UWBG semiconductors. (a) Absorption edge of β-Ga₂O₃. (b) The comparison between BSE and independent QP for optical spectra of β-Ga₂O₃. (c) Band gap and exciton binding energy of atomically thin GaN/AIN heterostructures. (d) Phonon-assisted optical absorption coefficient of silicon using second-order perturbations theory and the special displacement approach. (e) Lattice-screening effects on the optical spectra of In₂O₃. Panel (a) reprinted with permission from Ref. [39], Copyright 2019, AIP Publishing. Panel (b) reprinted with permission from Ref. [105], Copyright 2015, IOP Publishing. Panel (c) reprinted with permission from Ref. [106], Copyright 2019, AIP Publishing. Panel (d) reprinted with permission from Ref. [107], Copyright 2016, APS. Panel (e) reprinted from Ref. [108].

dissociated around room temperature. However, exciton binding tends to amplify with increasing band gap into the UWBG regime, and becomes particularly strong in quantum-confined heterostructures in which Coulomb effects are enhanced by the reduced dimensionality. For example, excitonic calculations in atomically thin GaN quantum wells embedded in Al(Ga)N barriers demonstrated that the strong quantum confinement effect results in a large enhancement of the exciton binding energy up to 216 meV, resulting in excitonic emission at room temperature that may increase the internal quantum efficiency (Fig. 9c) [106, 110, 111]. Excitonic effects are also strong in hexagonal boron nitride (h-BN), with a binding energy of ~ 700 meV [112, 113], which also demonstrates enhanced electron–hole interactions due to its layered crystal structure.

Despite these successes, several methodological challenges remain that limit our predictive understanding of the optical properties of UWBG materials. For realistic room-temperature applications it is important to consider the effect of phonons on the optical and excitonic properties of semiconductors [114]. This is especially true for indirect-gap materials, in which momentum transfer from phonons to electrons enables optical transitions across the fundamental indirect gap. Such higher-order processes are computationally demanding to evaluate,

but novel first-principles approaches for the study of phononmediated optical phenomena have emerged in recent years, e.g., the phonon-assisted optical absorption spectrum of indirectgap semiconductors can be calculated with methods based on second-order perturbation theory [115] or finite displacements of the atoms derived from eigenvalues and eigenmodes of the dynamical matrix (Fig. 9d) [116, 117]. In the reverse process, phonon-assisted transitions enable luminescence in indirectgap materials, and calculations have been applied to study the phonon-assisted luminescence of excitons in h-BN based on finite differences [118, 119] or density-functional perturbation theory, finding excellent agreement with the experimental spectra. Phonons also contribute to the screening of the electron-hole Coulomb interactions [120], and the study of such effects from first principles is still in its early stages. Simple models have been employed to take into account lattice-screening effects on excitons [108, 121] and found good agreement with the experiment (Fig. 9e). Further work along the lines of a recent study on exciton-phonon interactions in 2D materials from first principles [122] will help elucidate the role of phonons on the excitonic properties of UWBG semiconductors. In addition, excitonic corrections can have a giant effect on the non-linear optical response [123] and



need to be considered to understand non-linear electron-photon interactions in UWBG materials.

Radiative and non-radiative recombination

Carrier recombination in semiconductors occurs when excited electrons and holes introduced into the active region annihilate with each other and release their excess energy as heat or light. This recombination can be desirable, e.g., in optoelectronic devices where it is necessary for light emission, or undesirable, e.g., in solar cells and transistors where it is a pathway for energy loss. Understanding and predicting the recombination rates from first principles is important in uncovering the microscopic origins of energy loss in ultra-wide-band-gap semiconductor devices, especially since non-radiative processes do not generate a signal and are thus difficult to study experimentally. Calculations of recombination rates in wide-band-gap InGaN materials have provided fruitful insights in the efficiency of visible optoelectronic devices, and can play an important role in identifying the source of the low efficiency of ultra-wide-bandgap UV LEDs.

In the non-radiative Shockley–Read–Hall (SRH) process, an electron (hole) is captured by a defect level located within the band gap, followed by the subsequent capture of a hole (electron) by the same defect. The carrier capture is mediated by multi-phonon emission which ensures energy conservation before and after the electronic transition. Calculations of capture coefficients from first principles were performed by Shi and Wang using the adiabatic-coupling theory for the $\rm Zn_{\rm Ga}\it V_{\rm N}$

complex in GaN [127]. Later, Alkauskas et al. developed a methodology based on the static-coupling theory, which uses the wave function for a carefully chosen atomic geometry as the starting point for perturbation theory, that has been applied to identify a variety of candidate defects in the nitrides that act as efficient SRH centers [128-131]. Finally, Barmparis et al. have developed a first-principles formalism to treat inelastic scattering and carrier capture by defects, which they subsequently applied to calculate the capture cross section of a hydrogenated vacancy complex in Si [84]. Figure 10a shows an example of such a calculation for a gallium-vacancy complex with oxygen in GaN. The SRH recombination rate depends exponentially on the charge-transition level of the defect with respect to the band edges. Despite the improved accuracy of GW and HSE calculations, it remains useful to present the total recombination rate as a function of the adjusted band gap to account for possible deviations from experiment that sensitively affect the SRH coefficient. Moreover, rigidly shifting the band gap by a constant value to match experiment is a computationally efficient method to simulate SRH recombination in alloys, as such calculations are computationally demanding in alloy supercells.

In the radiative process, an electron and a hole recombine via the spontaneous emission of a photon. The simplest way of calculating the recombination rate is by Fermi's golden rule, treating the electromagnetic field semi-classically and evaluating the dipole transition matrix elements using the single-particle DFT wave functions. This has been performed successfully by Kioupakis et al. to calculate the radiative recombination coefficient as a function of temperature and carrier density for bulk

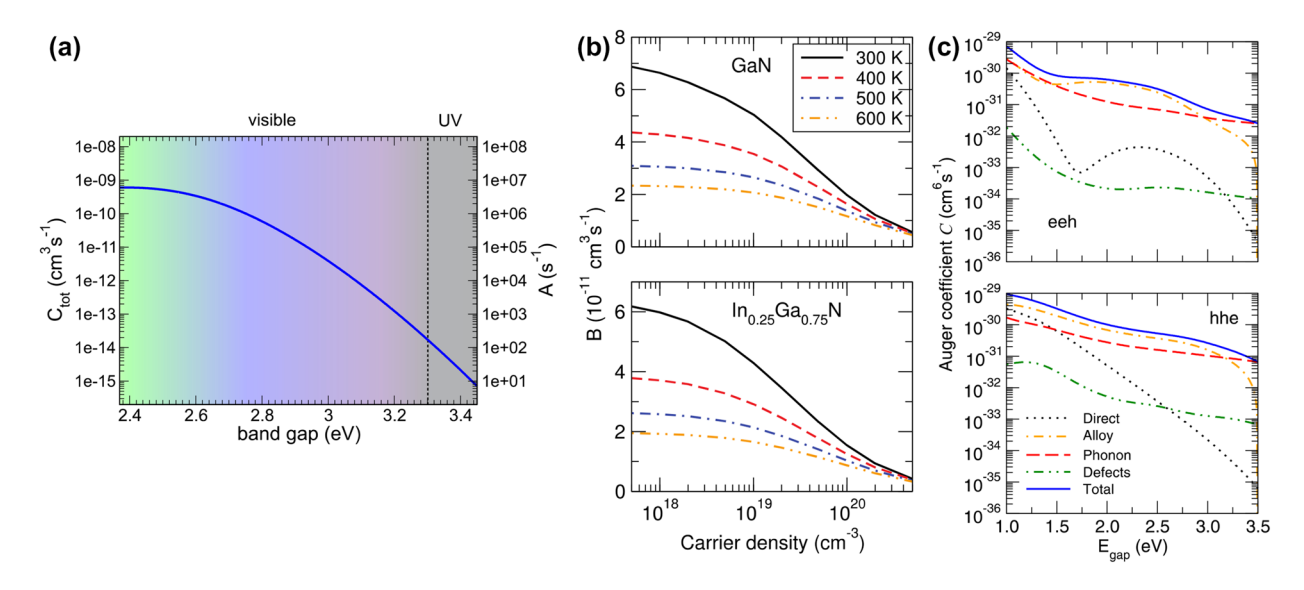


Figure 10: First-principles calculations of carrier recombination coefficients in the nitrides. (a) Total capture coefficient (left) and Shockley–Read–Hall recombination coefficient (for a defect density of 10^{16} cm⁻³) of a gallium-vacancy complex with oxygen in InGaN as a function of the band gap. (b) The radiative coefficient as a function of carrier density for GaN (top) and InGaN (bottom). (c) The Auger recombination coefficient of InGaN for the electron–electron–hole (top) and hole–hole–electron (bottom) processes. Panel (a) reprinted with permission from Ref. [124], Copyright 2016, APS. Panel (b) reprinted from Ref. [125]. Panel (c) reprinted with permission from Ref. [126], Copyright 2015, APS.



(In)GaN in good agreement with experiment (Fig. 10b) [125]. This methodology can be further extended to phonon-assisted optical transitions, which is required to explain the luminescence characteristics of indirect-gap semiconductors (see section on Optical Properties and Excitons above). A drawback of this approach is that it ignores electron-hole correlations, which may increase the recombination rate [132]. Recently developed approaches that treat the Coulomb effects based on the Bethe–Salpeter equation (see section on Optical Properties and Excitons above) and account for exciton dissociation are in good agreement with the low-temperature experimental radiative lifetimes [133].

In the Auger process, an electron and hole recombine while transferring their excess energy to another electron or hole via the Coulomb interaction. Auger rates are also calculated via Fermi's golden rule in combination with DFT energies and wave functions [126, 132, 134]. Additional scattering mechanisms due to alloy disorder or phonons are accounted for with supercell or density-functional perturbation theory, respectively. Firstprinciples calculations have been instrumental in identifying Auger recombination as the source of efficiency drop in InGaNbased LEDs. Although conventional wisdom suggests that Auger recombination is only important for narrow-gap materials, predictive calculations by Kioupakis et al. identified indirect Auger recombination, assisted by phonons and alloy disorder, as being dominant in the wide-band-gap InGaN system (Fig. 10c) [126, 132]. Similar to the SRH rate, the Auger rate depends sensitively on the magnitude of the band gap. As such, band-structure calculations based on many-body perturbation theory have been successfully applied to calculate the Auger rates in, e.g., bulk InN and NaI [135, 136].

Current challenges associated with recombination-rate calculations with DFT relate to the system size/complexity and to the inclusion of many-body effects. Since DFT can typically handle supercells up to the order of 100–1000 atoms, most studies have focused on bulk materials. However, carrier confinement in quantum-well heterostructures and carrier localization by composition fluctuations in alloys enables recombination processes that are symmetry-forbidden in the bulk [19, 137]. These calculations of alloys and heterostructures require supercells with > 10,000 atoms [53]. Such calculations, which rely on semiempirical techniques such as empirical tight binding, empirical pseudopotential, or modified $k \cdot p$ methods, have been used to study radiative and Auger recombination in disordered systems and in quantum wells [19, 138, 139]. Developments in real-space DFT methods, which can handle systems with ~ 100,000 electrons, could make it possible to predictively calculate recombination rates in large simulation cells, thereby resolving the open questions regarding the effects of heterostructure confinement and localization [140]. Another challenge is the systematic inclusion of many-body effects. Excitonic effects have been considered for the case of radiative recombination [106, 133], but their effect on SRH or Auger recombination rates remain less explored from first principles. Calculations of Auger rates with excitonic and biexcitonic corrections have been realized by, e.g., Philbin and Rabani based on the empirical pseudopotential method [141]. The inclusion of such higher-order bound states is necessary to understand carrier recombination in novel ultra-wide-band-gap nitride light emitters such as atomically thin GaN [106, 110, 111].

High-throughput calculations and computational discovery

In addition to theoretically characterizing the properties of known UWBG compounds, the inherently predictive nature of DFT calculations enables them to computationally discover new promising UWBG semiconducting materials and guide experimental studies. For example, numerous members of the II-IV nitride family of compounds (e.g., ZnGeN₂) are being investigated as alternatives to the group-III nitrides for UWBG semiconducting applications. DFT and related techniques have been applied to understand the electronic structure and defect properties of II-IV nitrides, including the effects of compositional disorder of the cation sublattice on the band gap [142]. Computational studies based on DFT have also uncovered semiconducting properties in previously unexplored materials such as the prediction of shallow donors in LiGaO₂ [143], the possibility of p-type doping in metastable rocksalt ZnO [144], and the formation of 2DEGs in the epsilon phase of Ga₂O₃ [17]. DFT calculations also revealed that the rutile phase of GeO2 is an UWBG semiconductor that overcomes several of the limitations of β-Ga₂O₃ due to its predicted ambipolar dopability, higher carrier mobilities, and higher thermal conductivity [145]. These examples demonstrate how DFT studies can be applied before experimental techniques to assess the feasibility of materials for UWBG semiconducting applications.

Moreover, a distinct advantage of computational techniques is that they can be deployed at scale by leveraging high-throughput calculations and materials-informatics techniques. DFT materials data have been calculated for tens of thousands of materials and made openly accessible in materials-genome databases such as the Materials Project [146], which can be mined to identify as-yet unexplored UWBG semiconductors. Such techniques have been applied to, e.g., discover new thermoelectric and transparent conducting materials among the entire materials genome [147]. In addition, materials databases have been combined with analytical models for carrier transport and breakdown to identify candidate materials with a high Baliga figure of merit for power electronics [148]. Similar techniques could be applied to predict new UWBG semiconductors



for targeted applications such as ambipolar dopability or efficient deep-UV light emissions.

Yet, despite these successes several open challenges still remain with theoretical materials discovery. Although targeted studies tend to focus on a limited set of materials features (e.g., the dopability or the carrier mobility), the feasibility of a material in semiconductor device applications also needs to consider the challenges with its growth in high-quality thin-film form, such as the availability of substrates, the competition with other unfavorable crystalline or amorphous phases, and the occurrence of unintentional defects that may hinder the conductivity. For high-throughput and materials-informatics studies, a set of challenges revolves around the accuracy of available database parameters, as they are most often obtained with less accurate DFT functionals such as PBE. This is particularly important for band gaps, which are severely underestimated by PBE, and for carrier effective masses, since they are critical in determining the material dopability and carrier transport. In that area, the recent availability of accurate band-gap data obtained with hybrid functionals [149], and the development of techniques to determine accurate carrier scattering rates at scale [150] are promising new avenues that will enable the efficient discovery of new candidate UWBG semiconductors.

Conclusions

In summary, we present a survey of computational techniques based on DFT that aim to predict and understand the properties of UWBG semiconductors. We highlight key results from the literature that successfully addressed open questions in UWBG semiconductor research, and we identify open questions for method development to further advance the field. Our review illustrates how DFT techniques have evolved into an indispensable materials characterization tool that can support, complement, and guide experimental studies with the goal to improve the performance of devices and to discover new materials that surpass the current state of the art.

Acknowledgments

This work was supported as part of the Computational Materials Sciences Program funded by the U.S. Department of Energy, Office of Science, Basic Energy Sciences, under Award No. DE-SC0020129. K.B. also acknowledges that this material is based upon work supported by the U.S. Department of Energy, Office of Science, Office of Advanced Scientific Computing Research, Department of Energy Computational Science Graduate Fellowship under Award Number DE-SC0020347. W.L. was partially supported by the Kwanjeong Educational Foundation Scholarship. N.P. gratefully acknowledges the support of the

Natural Sciences and Engineering Research Council of Canada (NSERC) Postgraduate Doctoral Scholarship. S.C. acknowledges the support provided by the Rackham Predoctoral Fellowship.

Funding

Basic Energy Sciences, DE-SC0020129, Emmanouil Kioupakis, Advanced Scientific Computing Research, DE-SC0020347, Kyle Bushick, Natural Sciences and Engineering Research Council of Canada, Horace H. Rackham School of Graduate Studies, University of Michigan

Declarations

Conflict of interest The authors declare no conflicts of interest.

References

- J.Y. Tsao, S. Chowdhury, M.A. Hollis, D. Jena, N.M. Johnson, K.A. Jones, R.J. Kaplar, S. Rajan, C.G. Van de Walle, E. Bellotti, C.L. Chua, R. Collazo, M.E. Coltrin, J.A. Cooper, K.R. Evans, S. Graham, T.A. Grotjohn, E.R. Heller, M. Higashiwaki, M.S. Islam, P.W. Juodawlkis, M.A. Khan, A.D. Koehler, J.H. Leach, U.K. Mishra, R.J. Nemanich, R.C.N. Pilawa-Podgurski, J.B. Shealy, Z. Sitar, M.J. Tadjer, A.F. Witulski, M. Wraback, J.A. Simmons, Ultrawide-bandgap semiconductors: research opportunities and challenges. Adv. Electron. Mater. 4(1), 1 (2018)
- 2. A. Kyrtsos, M. Matsubara, E. Bellotti, First-principles study of the impact of the atomic configuration on the electronic properties of $Al_xGa_{1-x}N$ alloys. Phys. Rev. B **99**, 035201 (2019)
- 3. H. Peelaers, J.B. Varley, J.S. Speck, C.G. Van de Walle, Structural and electronic properties of ${\rm Ga_2O_3\text{-}Al_2O_3}$ alloys. Appl. Phys. Lett. 112, 242101 (2018)
- F. Giustino, Materials Modelling Using Density Functional Theory: Properties and Predictions (Oxford University Press, New York, 2014)
- N. Marzari, A. Ferretti, C. Wolverton, Electronic-structure methods for materials design. Nat. Mater. 20(6), 736 (2021)
- 6. P. Giannozzi, O. Andreussi, T. Brumme, O. Bunau, M. Buongiorno Nardelli, M. Calandra, R. Car, C. Cavazzoni, D. Ceresoli, M. Cococcioni, N. Colonna, I. Carnimeo, A. Dal Corso, S. De Gironcoli, P. Delugas, R.A. Distasio, A. Ferretti, A. Floris, G. Fratesi, G. Fugallo, R. Gebauer, U. Gerstmann, F. Giustino, T. Gorni, J. Jia, M. Kawamura, H.Y. Ko, A. Kokalj, E. Kücükbenli, M. Lazzeri, M. Marsili, N. Marzari, F. Mauri, N.L. Nguyen, H.V. Nguyen, A. Otero-De-La-Roza, L. Paulatto, S. Poncé, D. Rocca, R. Sabatini, B. Santra, M. Schlipf, A.P. Seitsonen, A. Smogunov, I. Timrov, T. Thonhauser, P. Umari, N. Vast, X. Wu, S. Baroni, Advanced capabilities for materials modelling with Quantum ESPRESSO. J. Phys. Condens. Matter 29, 465901 (2017).



- A.H. Romero, D.C. Allan, B. Amadon, G. Antonius, T. Applencourt, L. Baguet, J. Bieder, F. Bottin, J. Bouchet, E. Bousquet, F. Bruneval, G. Brunin, D. Caliste, M. Côté, J. Denier, C. Dreyer, P. Ghosez, M. Giantomassi, Y. Gillet, O. Gingras, D.R. Hamann, G. Hautier, F. Jollet, G. Jomard, A. Martin, H.P.C. Miranda, F. Naccarato, G. Petretto, N.A. Pike, V. Planes, S. Prokhorenko, T. Rangel, F. Ricci, G.M. Rignanese, M. Royo, M. Stengel, M. Torrent, M.J. Van Setten, B. Van Troeye, M.J. Verstraete, J. Wiktor, J.W. Zwanziger, X. Gonze, ABINIT: overview and focus on selected capabilities. J. Chem. Phys. 152, 124102 (2020)
- J. Hafner, Ab-initio simulations of materials using VASP: density-functional theory and beyond. J. Comput. Chem. 29, 2044 (2008)
- 9. D.M. Ceperley, B.J. Alder, Ground state of the electron gas by a stochastic method. Phys. Rev. Lett. **45**(7), 566 (1980)
- J. Perdew, A. Zunger, Self-interaction correction to densityfunctional approximations for many-electron systems. Phys. Rev. B 23(10), 5048 (1981)
- J. Perdew, K. Burke, M. Ernzerhof, Generalized gradient approximation made simple. Phys. Rev. Lett. 77(18), 3865 (1996)
- 12. A. van de Walle, M. Asta, G. Ceder, The alloy theoretic automated toolkit: a user guide. Calphad **26**(4), 539 (2002)
- J. Heyd, G.E. Scuseria, M. Ernzerhof, Erratum: "Hybrid functionals based on a screened Coulomb potential" [J. Chem. Phys. 118, 8207 (2003)]. J. Chem. Phys. 124(21), 219906 (2006).
- L. Lymperakis, J. Neugebauer, Large anisotropic adatom kinetics on nonpolar GaN surfaces: consequences for surface morphologies and nanowire growth. Phys. Rev. B 79(24), 241308 (2009)
- 15. R. King-Smith, D. Vanderbilt, Theory of polarization of crystalline solids. Phys. Rev. B **47**(3), 1651 (1993)
- C.E. Dreyer, A. Janotti, C.G. Van de Walle, D. Vanderbilt,
 Correct implementation of polarization constants in wurtzite
 materials and impact on III-nitrides. Phys. Rev. X 6(2), 021038
 (2016)
- 17. S.B. Cho, R. Mishra, Epitaxial engineering of polar ϵ -Ga₂O₃ for tunable two-dimensional electron gas at the heterointerface. Appl. Phys. Lett. **112**, 162101 (2018)
- N.L. Adamski, C.E. Dreyer, C.G. Van de Walle, Giant polarization charge density at lattice-matched GaN/ScN interfaces.
 Appl. Phys. Lett. 115, 232103 (2019)
- C.M. Jones, C.H. Teng, Q. Yan, P.C. Ku, E. Kioupakis, Impact of carrier localization on recombination in InGaN quantum wells and the efficiency of nitride light-emitting diodes: insights from theory and numerical simulations. Appl. Phys. Lett. 111, 113501 (2017)
- K. Lejaeghere, G. Bihlmayer, T. Björkman, P. Blaha, S. Blügel,
 V. Blum, D. Caliste, I.E. Castelli, S.J. Clark, A. Dal Corso,
 S. De Gironcoli, T. Deutsch, J.K. Dewhurst, I. Di Marco, C.
 Draxl, M. Dułak, O. Eriksson, J.A. Flores-Livas, K.F. Garrity,
 L. Genovese, P. Giannozzi, M. Giantomassi, S. Goedecker,

- X. Gonze, O. Grånäs, E.K.U. Gross, A. Gulans, F. Gygi, D.R. Hamann, P.J. Hasnip, N.A.W. Holzwarth, D. Iuşan, D.B. Jochym, F. Jollet, D. Jones, G. Kresse, K. Koepernik, E. Küçükbenli, Y.O. Kvashnin, I.L.M. Locht, S. Lubeck, M. Marsman, N. Marzari, U. Nitzsche, L. Nordström, T. Ozaki, L. Paulatto, C.J. Pickard, W. Poelmans, M.I.J. Probert, K. Refson, M. Richter, G.M. Rignanese, S. Saha, M. Scheffler, M. Schlipf, K. Schwarz, S. Sharma, F. Tavazza, P. Thunström, A. Tkatchenko, M. Torrent, D. Vanderbilt, M.J. Van Setten, V. Van Speybroeck, J.M. Wills, J.R. Yates, G.X. Zhang, S. Cottenier, Reproducibility in density functional theory calculations of solids. Science 351, 1415 (2016)
- J. Sun, A. Ruzsinszky, J. Perdew, Strongly constrained and appropriately normed semilocal density functional. Phys. Rev. Lett. 115, 036402 (2015)
- 22. K.A. Mengle, E. Kioupakis, Vibrational and electron-phonon coupling properties of β -Ga₂O₃ from first-principles calculations: impact on the mobility and breakdown field. AIP Adv. **9**, 015313 (2019)
- J. Carrete, B. Vermeersch, A. Katre, A. van Roekeghem, T. Wang, G.K.H. Madsen, N. Mingo, almaBTE: a solver of the space–time dependent Boltzmann transport equation for phonons in structured materials. Comput. Phys. Commun. 220, 351 (2017)
- S. Baroni, S. de Gironcoli, A. Dal Corso, P. Giannozzi, Phonons and related crystal properties from density-functional perturbation theory. Rev. Mod. Phys. 73(2), 515 (2001)
- 25. C. Verdi, F. Giustino, Fröhlich electron-phonon vertex from first principles. Phys. Rev. Lett. **115**, 176401 (2015)
- A. Togo, I. Tanaka, First principles phonon calculations in materials science. Scr. Mater. 108, 1 (2015)
- 27. J.H. Lloyd-Williams, B. Monserrat, Lattice dynamics and electron-phonon coupling calculations using nondiagonal supercells. Phys. Rev. B **92**, 184301 (2015)
- L. Lindsay, A. Katre, A. Cepellotti, N. Mingo, Perspective on ab initio phonon thermal transport. J. Appl. Phys. 126, 050902 (2019)
- 29. M.D. Santia, N. Tandon, J.D. Albrecht, Lattice thermal conductivity in β -Ga $_2$ O $_3$ from first principles. Appl. Phys. Lett. 107, 041907 (2015)
- S. Mu, H. Peelaers, C.G. Van de Walle, Ab initio study of enhanced thermal conductivity in ordered AlGaO₃ alloys. Appl. Phys. Lett. 115, 242103 (2019)
- L. Lindsay, D.A. Broido, T.L. Reinecke, First-principles determination of ultrahigh thermal conductivity of boron arsenide: a competitor for diamond? Phys. Rev. Lett. 111, 025901 (2013)
- K. Chen, B. Song, N.K. Ravichandran, Q. Zheng, X. Chen, H.
 Lee, H. Sun, S. Li, G.A.G.U. Gamage, F. Tian, Z. Ding, Q. Song,
 A. Rai, H. Wu, P. Koirala, A.J. Schmidt, K. Watanabe, B. Lv,
 Z. Ren, L. Shi, D.G. Cahill, T. Taniguchi, D. Broido, G. Chen,



- Ultrahigh thermal conductivity in isotope-enriched cubic boron nitride. Science **367**, 555 (2020)
- A.H. Romero, E.K.U. Gross, M.J. Verstraete, O. Hellman, Thermal conductivity in PbTe from first principles. Phys. Rev. B 91, 214310 (2015)
- F. Tian, B. Song, X. Chen, N.K. Ravichandran, Y. Lv, Z. Ding,
 J. Sun, G. Amila, G. Udalamatta, H. Sun, S. Chen, C. Chu, P.Y.
 Huang, D. Broido, L. Shi, Unusual high thermal conductivity
 in boron arsenide bulk crystals. Science 361, 582 (2018)
- S. Dagli, K.A. Mengle, E. Kioupakis, Thermal conductivity of AlN, GaN, and Al_xGa_{1-x}N alloys as a function of composition, temperature, crystallographic direction, and isotope disorder from first principles. arXiv 1910.05440 (2019).
- M. Simoncelli, N. Marzari, F. Mauri, Unified theory of thermal transport in crystals and glasses. Nat. Phys. 15(8), 809 (2019)
- R.J. Kaplar, O. Slobodyan, J.D. Flicker, M.A. Hollis, A new analysis of the dependence of critical electric field on semiconductor bandgap. ECS Meet. Abstr. MA2019-02, 1334 (2019).
- P. Rinke, M. Winkelnkemper, A. Qteish, D. Bimberg, J. Neugebauer, M. Scheffler, Consistent set of band parameters for the group-III nitrides AlN, GaN, and InN. Phys. Rev. B 77(7), 075202 (2008)
- 39. K.A. Mengle, G. Shi, D. Bayerl, E. Kioupakis, First-principles calculations of the near-edge optical properties of β -Ga₂O₃. Appl. Phys. Lett. **109**(21), 212104 (2016)
- P.G. Moses, M. Miao, Q. Yan, C.G. Van de Walle, Hybrid functional investigations of band gaps and band alignments for AlN, GaN, InN, and InGaN. J. Chem. Phys. 134(8), 084703 (2011)
- 41. A. Kyrtsos, M. Matsubara, E. Bellotti, Band offsets of $Al_xGa_{1-x}N$ alloys using first-principles calculations. J. Phys. Condens. Matter **32**(36), 365504 (2020)
- 42. S. Poncé, Y. Gillet, J. Laflamme Janssen, A. Marini, M. Verstraete, X. Gonze, Temperature dependence of the electronic structure of semiconductors and insulators. J. Chem. Phys. **143**(10), 102813 (2015)
- 43. M.L. Tiago, S. Ismail-Beigi, S.G. Louie, Effect of semicore orbitals on the electronic band gaps of Si, Ge, and GaAs within the GW approximation. Phys. Rev. B **69**, 125212 (2004)
- J. Deslippe, G. Samsonidze, D.A. Strubbe, M. Jain, M.L. Cohen, S.G. Louie, BerkeleyGW: a massively parallel computer package for the calculation of the quasiparticle and optical properties of materials and nanostructures. Comput. Phys. Commun. 183(6), 1269 (2012)
- 45. D. Wing, J.B. Haber, R. Noff, B. Barker, D.A. Egger, A. Ramasubramaniam, S.G. Louie, J.B. Neaton, L. Kronik, Comparing time-dependent density functional theory with many-body perturbation theory for semiconductors: screened range-separated hybrids and the GW plus Bethe-Salpeter approach. Phys. Rev. Mater. 3, 064603 (2019)

- 46. T. Rangel, M. Del Ben, D. Varsano, G. Antonius, F. Bruneval, F.H. da Jornada, M.J. van Setten, O.K. Orhan, D.D. O'Regan, A. Canning, A. Ferretti, A. Marini, G.M. Rignanese, J. Deslippe, S.G. Louie, J.B. Neaton, Reproducibility in G0W0 calculations for solids. Comput. Phys. Commun. 255, 107242 (2020)
- Q. Yan, P. Rinke, M. Scheffler, C.G. Van de Walle, Strain effects in group-III nitrides: deformation potentials for AlN, GaN, and InN. Appl. Phys. Lett. 95(12), 121111 (2009)
- C.G. Van de Walle, R. Martin, Theoretical study of band offsets at semiconductor interfaces. Phys. Rev. B 35, 8154 (1987)
- C.G. Van de Walle, J. Neugebauer, Universal alignment of hydrogen levels in semiconductors, insulators and solutions. Nature 423(6940), 626 (2003)
- A. Schleife, F. Fuchs, C. Rödl, J. Furthmüller, F. Bechstedt, Branch-point energies and band discontinuities of III-nitrides and III-/II-oxides from quasiparticle band-structure calculations. Appl. Phys. Lett. 94(1), 012104 (2009)
- F. Giustino, S.G. Louie, M.L. Cohen, Electron-phonon renormalization of the direct band gap of diamond. Phys. Rev. Lett. 105(26), 265501 (2010)
- M. Zacharias, M. Scheffler, C. Carbogno, Fully anharmonic nonperturbative theory of vibronically renormalized electronic band structures. Phys. Rev. B 102(4), 045126 (2020)
- D. Chaudhuri, M. Odonovan, T. Streckenbach, O. Marquardt, P. Farrell, S.K. Patra, T. Koprucki, S. Schulz, Multiscale simulations of the electronic structure of III-nitride quantum wells with varied indium content: connecting atomistic and continuum-based models. J. Appl. Phys. 129(7), 073104 (2021)
- L. Gordon, J.L. Lyons, A. Janotti, C.G. VandeWalle, Hybrid functional calculations of DX centers in AlN and GaN. Phys. Rev. B 89(8), 085204 (2014)
- A. Pandey, X. Liu, Z. Deng, W.J. Shin, D.A. Laleyan, K. Mashooq, E.T. Reid, E. Kioupakis, P. Bhattacharya, Z. Mi, Enhanced doping efficiency of ultrawide band gap semiconductors by metal-semiconductor junction assisted epitaxy. Phys. Rev. Mater. 3, 053401 (2019)
- Y. Wu, D.A. Laleyan, Z. Deng, C. Ahn, A.F. Aiello, A. Pandey, X. Liu, P. Wang, K. Sun, E. Ahmadi, Y. Sun, M. Kira, P.K. Bhattacharya, E. Kioupakis, Z. Mi, controlling defect formation of nanoscale AlN: toward efficient current conduction of ultrawide-bandgap semiconductors. Adv. Electron. Mater. 6, 2000337 (2020)
- L. Weston, D. Wickramaratne, C.G. Van de Walle, Hole polarons and p -type doping in boron nitride polymorphs. Phys. Rev. B 96, 100102 (2017)
- E. Kioupakis, P. Rinke, C.G. Van de Walle, Determination of internal loss in nitride lasers from first principles. Appl. Phys. Express 3, 082101 (2010)
- J.L. Lyons, D. Wickramaratne, C.G. Van de Walle, A first-principles understanding of point defects and impurities in GaN. J. Appl. Phys. 129, 111101 (2021)



- C. Freysoldt, J. Neugebauer, C.G. Van de Walle, Fully ab initio finite-size corrections for charged-defect supercell calculations. Phys. Rev. Lett. 102, 016402 (2009)
- Á. Szabó, N.T. Son, E. Janźn, A. Gali, Group-II acceptors in wurtzite AlN: a screened hybrid density functional study. Appl. Phys. Lett. 96, 192110 (2010)
- J.L. Lyons, A. Janotti, C.G. Van de Walle, Shallow versus deep nature of Mg acceptors in nitride semiconductors. Phys. Rev. Lett. 108(15), 156403 (2012)
- 63. C. Stampfl, J. Neugebauer, C.G. Van de Walle, Doping of Al_xGa_{1-x}N alloys. Mater. Sci. Eng. B **59**(1–3), 253 (1999)
- 64. Z. Bryan, I. Bryan, B.E. Gaddy, P. Reddy, L. Hussey, M. Bobea, W. Guo, M. Hoffmann, R. Kirste, J. Tweedie, M. Gerhold, D.L. Irving, Z. Sitar, R. Collazo, Fermi level control of compensating point defects during metalorganic chemical vapor deposition growth of Si-doped AlGaN. Appl. Phys. Lett. 105(22), 222101 (2014)
- P. Reddy, M.P. Hoffmann, F. Kaess, Z. Bryan, I. Bryan, M. Bobea, A. Klump, J. Tweedie, R. Kirste, S. Mita, M. Gerhold, R. Collazo, Z. Sitar, Point defect reduction in wide bandgap semiconductors by defect quasi Fermi level control. J. Appl. Phys. 120, 185704 (2016)
- 66. M.W. Swift, H. Peelaers, S. Mu, J.J.L. Morton, C.G. Van de Walle, First-principles calculations of hyperfine interaction, binding energy, and quadrupole coupling for shallow donors in silicon. npj Comput. Mater. 6, 181 (2020)
- S. Poncé, D. Jena, F. Giustino, Route to high hole mobility in GaN via reversal of crystal-field splitting. Phys. Rev. Lett. 123, 096602 (2019)
- 68. K. Ghosh, U. Singisetti, Ab initio calculation of electron-phonon coupling in monoclinic β -Ga $_2$ O $_3$ crystal. Appl. Phys. Lett. 109, 072102 (2016)
- N. Pant, Z. Deng, E. Kioupakis, High electron mobility of Al_xGa_{1-x}N evaluated by unfolding the DFT band structure. Appl. Phys. Lett. 117, 242105 (2020)
- N. Sanders, E. Kioupakis, Phonon- and defect-limited electron and hole mobility of diamond and cubic boron nitride: a critical comparison. Appl. Phys. Lett. 119, 062101 (2021)
- O.D. Restrepo, K. Varga, S.T. Pantelides, First-principles calculations of electron mobilities in silicon: phonon and Coulomb scattering. Appl. Phys. Lett. 94, 212103 (2009)
- 72. F. Giustino, J.R. Yates, I. Souza, M.L. Cohen, S.G. Louie, Electron-phonon interaction via electronic and lattice Wannier functions: superconductivity in boron-doped diamond reexamined. Phys. Rev. Lett. 98(4), 047005 (2007)
- S. Poncé, E.R. Margine, F. Giustino, Towards predictive manybody calculations of phonon-limited carrier mobilities in semiconductors. Phys. Rev. B 97, 121201 (2018)
- J.J. Zhou, J. Park, I. Te Lu, I. Maliyov, X. Tong, M. Bernardi,
 PERTURBO: a software package for ab initio electron–phonon

- interactions, charge transport and ultrafast dynamics. Comput. Phys. Commun. **264**, 107970 (2021)
- G. Brunin, H.P.C. Miranda, M. Giantomassi, M. Royo, M. Stengel, M.J. Verstraete, X. Gonze, G.M. Rignanese, G. Hautier, Electron-phonon beyond Fröhlich: dynamical quadrupoles in polar and covalent solids. Phys. Rev. Lett. 125, 136601 (2020)
- V.A. Jhalani, J.J. Zhou, J. Park, C.E. Dreyer, M. Bernardi, Piezoelectric electron-phonon interaction from ab initio dynamical quadrupoles: impact on charge transport in Wurtzite GaN. Phys. Rev. Lett. 125, 136602 (2020)
- S. Poncé, W. Li, S. Reichardt, F. Giustino, First-principles calculations of charge carrier mobility and conductivity in bulk semiconductors and two-dimensional materials. Reports Prog. Phys. 83, 036501 (2020)
- V. Lordi, P. Erhart, D. Åberg, Charge carrier scattering by defects in semiconductors. Phys. Rev. B 81, 235204 (2010)
- I. Te Lu, J.J. Zhou, M. Bernardi, Efficient ab initio calculations of electron-defect scattering and defect-limited carrier mobility. Phys. Rev. Mater. 3, 033804 (2019)
- F. Murphy-Armando, S. Fahy, First-principles calculation of alloy scattering in Ge_xSi_{1-x}. Phys. Rev. Lett. 97, 096606 (2006)
- S. Poncé, D. Jena, F. Giustino, Hole mobility of strained GaN from first principles. Phys. Rev. B 100, 085204 (2019)
- 82. Y. Kang, K. Krishnaswamy, H. Peelaers, C.G. Van de Walle, Fundamental limits on the electron mobility of β -Ga₂O₃. J. Phys. Condens. Matter **29**, 234001 (2017)
- S. Poncé, F. Giustino, Structural, electronic, elastic, power, and transport properties of β–Ga₂O₃ from first principles.
 Phys. Rev. Res. 2, 033102 (2020)
- 84. G.D. Barmparis, Y.S. Puzyrev, X.G. Zhang, S.T. Pantelides, Theory of inelastic multiphonon scattering and carrier capture by defects in semiconductors: application to capture cross sections. Phys. Rev. B **92**, 214111 (2015)
- J. Singh, Electronic and Optoelectronic Properties of Semiconductor Structures (Cambridge University Press, Cambridge, 2003), pp. 312–344
- 86. E. Matioli, T. Palacios, Room-temperature ballistic transport in iii-nitride heterostructures. Nano Lett. **15**(2), 1070 (2015)
- 87. C. Franchini, M. Reticcioli, M. Setvin, U. Diebold, Polarons in materials. Nat. Rev. Mater. **6**, 560 (2021)
- J.B. Varley, A. Janotti, C. Franchini, C.G. Van de Walle, Role of self-trapping in luminescence and p-type conductivity of wide-band-gap oxides. Phys. Rev. B 85(8), 081109 (2012)
- S. Kokott, S.V. Levchenko, P. Rinke, M. Scheffler, First-principles supercell calculations of small polarons with proper account for long-range polarization effects. New J. Phys. 20, 033023 (2018)
- W.H. Sio, C. Verdi, S. Poncé, F. Giustino, Polarons from First Principles, without Supercells. Phys. Rev. Lett. 122, 246403 (2019)



- 91. Y.K. Frodason, K.M. Johansen, L. Vines, J.B. Varley, Self-trapped hole and impurity-related broad luminescence in β-Ga₂O₃. J. Appl. Phys. **127**, 075701 (2020)
- 92. W.H. Sio, C. Verdi, S. Poncé, F. Giustino, Ab initio theory of polarons: Formalism and applications. Phys. Rev. B **99**(23), 235139 (2019)
- 93. J. Fang, M.V. Fischetti, R.D. Schrimpf, R.A. Reed, E. Bellotti, S.T. Pantelides, Electron transport properties of Al_xGa_{1-x}N/ GaN transistors based on first-principles calculations and Boltzmann-equation Monte Carlo simulations. Phys. Rev. Appl. 11, 044045 (2019)
- K. Ghosh, U. Singisetti, Ab initio velocity-field curves in monoclinic β-Ga₂O₃. J. Appl. Phys. 122, 035702 (2017)
- N. Marzari, A.A. Mostofi, J.R. Yates, I. Souza, D. Vanderbilt, Maximally localized Wannier functions: theory and applications. Rev. Mod. Phys. 84(4), 1419 (2012)
- S. Poncé, E.R. Margine, C. Verdi, F. Giustino, EPW: Electronphonon coupling, transport and superconducting properties using maximally localized Wannier functions. Comput. Phys. Commun. 209, 116 (2016)
- 97. T. Kotani, M. van Schilfgaarde, Impact ionization rates for Si, GaAs, InAs, ZnS, and GaN in the GW approximation. Phys. Rev. B **81**, 125201 (2010)
- 98. K. Ghosh, U. Singisetti, Impact ionization in β -Ga₂O₃. J. Appl. Phys. **124**(8), 085707 (2018)
- Y. Sun, S.A. Boggs, R. Ramprasad, The intrinsic electrical breakdown strength of insulators from first principles. Appl. Phys. Lett. 101(13), 132906 (2012)
- 100. X. Tong, M. Bernardi, Toward precise simulations of the coupled ultrafast dynamics of electrons and atomic vibrations in materials. Phys. Rev. Res. 3, 023072 (2021)
- J.M. Rondinelli, E. Kioupakis, Predicting and designing optical properties of inorganic materials. Annu. Rev. Mater. Res. 45(1), 491 (2015)
- 102. M. Rohlfing, S.G. Louie, Electron-hole excitations and optical spectra from first principles. Phys. Rev. B **62**(8), 4927 (2000)
- 103. D. Sangalli, A. Ferretti, H. Miranda, C. Attaccalite, I. Marri, E. Cannuccia, P. Melo, M. Marsili, F. Paleari, A. Marrazzo, G. Prandini, P. Bonfà, M.O. Atambo, F. Affinito, M. Palummo, A. Molina-Sánchez, C. Hogan, M. Grüning, D. Varsano, A. Marini, Many-body perturbation theory calculations using the yambo code. J. Phys. Condens. Matter 31, 325902 (2019)
- 104. X. Zhang, S. Achilles, J. Winkelmann, R. Haas, A. Schleife, E. Di Napoli, Solving the Bethe-Salpeter equation on massively parallel architectures. Comput. Phys. Commun. 267, 108081 (2020)
- 105. J.B. Varley, A. Schleife, Bethe-Salpeter calculation of optical-absorption spectra of $\rm In_2O_3$ and $\rm Ga_2O_3$. Semicond. Sci. Technol. **30**(2), 024010 (2015)
- D. Bayerl, E. Kioupakis, Room-temperature stability of excitons and transverse-electric polarized deep-ultraviolet

- luminescence in atomically thin GaN quantum wells. Appl. Phys. Lett. **115**, 131101 (2019)
- 107. M. Zacharias, F. Giustino, One-shot calculation of temperaturedependent optical spectra and phonon-induced band-gap renormalization. Phys. Rev. B 94(7), 075125 (2016)
- 108. A. Schleife, M.D. Neumann, N. Esser, Z. Galazka, A. Gottwald, J. Nixdorf, R. Goldhahn, M. Feneberg, Optical properties of In₂O₃ from experiment and first-principles theory: influence of lattice screening. New J. Phys. 20, 053016 (2018)
- X. Zhang, A. Schleife, Nonequilibrium BN-ZnO: Optical properties and excitonic effects from first principles. Phys. Rev. B 97, 125201 (2018)
- D. Bayerl, S. Islam, C.M. Jones, V. Protasenko, D. Jena, E.
 Kioupakis, Deep ultraviolet emission from ultra-thin GaN/AlN heterostructures. Appl. Phys. Lett. 109(24), 241102 (2016)
- 111. A. Aiello, Y. Wu, A. Pandey, P. Wang, W. Lee, D. Bayerl, N. Sanders, Z. Deng, J. Gim, K. Sun, R. Hovden, E. Kioupakis, Z. Mi, P. Bhattacharya, Deep ultraviolet luminescence due to extreme confinement in monolayer GaN/Al(Ga)N nanowire and planar heterostructures. Nano Lett. 19, 7852 (2019)
- B. Arnaud, S. Lebègue, P. Rabiller, M. Alouani, Huge excitonic effects in layered hexagonal boron nitride. Phys. Rev. Lett. 96, 026402 (2006)
- 113. L. Schué, L. Sponza, A. Plaud, H. Bensalah, K. Watanabe, T. Taniguchi, F. Ducastelle, A. Loiseau, J. Barjon, Bright luminescence from indirect and strongly bound excitons in h-BN. Phys. Rev. Lett. 122, 067401 (2019)
- A. Marini, Ab initio finite-temperature excitons. Phys. Rev. Lett. 101(10), 106405 (2008)
- 115. J. Noffsinger, E. Kioupakis, C.G. Van de Walle, S.G. Louie, M.L. Cohen, Phonon-assisted optical absorption in silicon from first principles. Phys. Rev. Lett. 108, 167402 (2012)
- M. Zacharias, F. Giustino, Theory of the special displacement method for electronic structure calculations at finite temperature. Phys. Rev. Res. 2, 013357 (2020)
- 117. B. Monserrat, C.E. Dreyer, K.M. Rabe, Phonon-assisted optical absorption in $BaSnO_3$ from first principles. Phys. Rev. B **97**, 104310 (2018)
- E. Cannuccia, B. Monserrat, C. Attaccalite, Theory of phononassisted luminescence in solids: application to hexagonal boron nitride. Phys. Rev. B 99(8), 081109 (2019)
- 119. F. Paleari, H.P.C. Miranda, A. Molina-Sánchez, L. Wirtz, Exciton-phonon coupling in the ultraviolet absorption and emission spectra of bulk hexagonal boron nitride. Phys. Rev. Lett. 122(18), 187401 (2019)
- F. Bechstedt, Many-Body Approach to Electronic Excitations (Springer, Berlin, Heidelberg, 2015)
- M.R. Filip, J.B. Haber, J.B. Neaton, Phonon screening of excitons in semiconductors: halide Perovskites and beyond. Phys. Rev. Lett. 127, 067401 (2021)



- T.A. Huang, M. Zacharias, D.K. Lewis, F. Giustino, S. Sharifzadeh, Exciton-phonon interactions in monolayer germanium selenide from first principles. J. Phys. Chem. Lett. 12(15), 3802 (2021)
- 123. Y.-H. Chan, D.Y. Qiu, F.H. da Jornada, S.G. Louie, Giant exciton-enhanced shift currents and direct current conduction with subbandgap photo excitations produced by many-electron interactions. Proc. Natl. Acad. Sci. 118(25), e1906938118 (2021)
- 124. A. Alkauskas, C.E. Dreyer, J.L. Lyons, C.G. Van de Walle, Role of excited states in Shockley-Read-Hall recombination in wideband-gap semiconductors. Phys. Rev. B 93, 201304 (2016)
- E. Kioupakis, Q. Yan, D. Steiauf, C.G. Van de Walle, Temperature and carrier-density dependence of Auger and radiative recombination in nitride optoelectronic devices. New J. Phys. 15, 125006 (2013)
- E. Kioupakis, D. Steiauf, P. Rinke, K.T. Delaney, C.G. Van de Walle, First-principles calculations of indirect Auger recombination in nitride semiconductors. Phys. Rev. B 92, 035207 (2015)
- L. Shi, L.W. Wang, Ab initio calculations of deep-level carrier nonradiative recombination rates in bulk semiconductors. Phys. Rev. Lett. 109, 245501 (2012)
- 128. A. Alkauskas, Q. Yan, C.G. Van de Walle, First-principles theory of nonradiative carrier capture via multiphonon emission. Phys. Rev. B 90(7), 075202 (2014)
- 129. C.E. Dreyer, A. Alkauskas, J.L. Lyons, J.S. Speck, C.G. Van de Walle, Gallium vacancy complexes as a cause of Shockley-Read-Hall recombination in III-nitride light emitters. Appl. Phys. Lett. 108(14), 141101 (2016)
- 130. D. Wickramaratne, J.X. Shen, C.E. Dreyer, M. Engel, M. Marsman, G. Kresse, S. Marcinkevičius, A. Alkauskas, C.G. Van de Walle, Iron as a source of efficient Shockley-Read-Hall recombination in GaN. Appl. Phys. Lett. 109, 162107 (2016)
- J.-X. Shen, D. Wickramaratne, C.E. Dreyer, A. Alkauskas, E. Young, J.S. Speck, C.G. Van de Walle, Calcium as a nonradiative recombination center in InGaN. Appl. Phys. Express 10, 021001 (2017)
- 132. E. Kioupakis, P. Rinke, K.T. Delaney, C.G. Van de Walle, Indirect Auger recombination as a cause of efficiency droop in nitride light-emitting diodes. Appl. Phys. Lett. 98(16), 161107 (2011)
- V.A. Jhalani, H.Y. Chen, M. Palummo, M. Bernardi, Precise radiative lifetimes in bulk crystals from first principles: the case of wurtzite gallium nitride. J. Phys. Condens. Matter 32, 084001 (2020)
- 134. M. Govoni, I. Marri, S. Ossicini, Auger recombination in Si and GaAs semiconductors: ab initio results. Phys. Rev. B 84, 075215 (2011)
- A. Mcallister, D. Bayerl, E. Kioupakis, Radiative and Auger recombination processes in indium nitride. Appl. Phys. Lett. 112, 251108 (2018)

- A. McAllister, D. Åberg, A. Schleife, E. Kioupakis, Auger recombination in sodium-iodide scintillators from first principles.
 Appl. Phys. Lett. 106(14), 141901 (2015)
- 137. A. Polkovnikov, G. Zegrya, Phys. Rev. B 58, 4039 (1998)
- 138. F. Bertazzi, X. Zhou, M. Goano, G. Ghione, E. Bellotti, Auger recombination in InGaN/GaN quantum wells: a full-Brillouinzone study. Appl. Phys. Lett. **103**, 081106 (2013)
- 139. J.M. Mcmahon, D.S.P. Tanner, E. Kioupakis, S. Schulz, Atomistic analysis of radiative recombination rate, Stokes shift, and density of states in c-plane InGaN/GaN quantum wells. Appl. Phys. Lett. 116, 181104 (2020)
- 140. P. Motamarri, S. Das, S. Rudraraju, K. Ghosh, D. Davydov, V. Gavini, DFT-FE A massively parallel adaptive finite-element code for large-scale density functional theory calculations. Comput. Phys. Commun. 246, 106853 (2020)
- J.P. Philbin, E. Rabani, Electron-hole correlations govern auger recombination in nanostructures. Nano Lett. 18(12), 7889 (2018)
- 142. S. Lyu, D. Skachkov, K. Kash, E.W. Blanton, W.R.L. Lambrecht, Band gaps, band-offsets, disorder, stability region, and point defects in II-IV- N_2 semiconductors. Phys. Status Solidi **216**, 1800875 (2019)
- 143. K. Dabsamut, A. Boonchun, W.R.L. Lambrecht, First-principles study of n- and p-type doping opportunities in LiGaO $_2$. J. Phys. D **53**, 274002 (2020)
- A. Goyal, V. Stevanović, Metastable rocksalt ZnO is p-type dopable. Phys. Rev. Mater. 2, 084603 (2018)
- 145. S. Chae, K.A. Mengle, K. Bushick, J. Lee, N. Sandaers, Z. Deng, Z. Mi, P.F.P. Poudeu, H. Paik, J.T. Heron, E. Kioupakis, Towards the predictive discovery of ambipolarly dopable ultra-wide-band-gap semiconductors: the case of rutile GeO₂. Appl. Phys. Lett. 118, 260501 (2021)
- 146. A. Jain, S.P. Ong, G. Hautier, W. Chen, W.D. Richards, S. Dacek, S. Cholia, D. Gunter, D. Skinner, G. Ceder, K.A. Persson, Commentary: the materials project: a materials genome approach to accelerating materials innovation. APL Mater. 1, 011002 (2013)
- 147. G. Hautier, Finding the needle in the haystack: materials discovery and design through computational ab initio high-throughput screening. Comput. Mater. Sci. 163, 108 (2019)
- 148. P. Gorai, R.W. McKinney, N.M. Haegel, A. Zakutayev, V. Stevanovic, A computational survey of semiconductors for power electronics. Energy Environ. Sci. **12**(11), 3338 (2019)
- 149. S. Kim, M. Lee, C. Hong, Y. Yoon, H. An, D. Lee, W. Jeong, D. Yoo, Y. Kang, Y. Youn, S. Han, A band-gap database for semiconducting inorganic materials calculated with hybrid functional. Sci. Data 7, 387 (2020)
- A.M. Ganose, J. Park, A. Faghaninia, R. Woods-Robinson, K.A.
 Persson, A. Jain, Efficient calculation of carrier scattering rates from first principles. Nat. Commun. 12, 2222 (2021)